Energy Conversion and Management: X 25 (2025) 100841

Contents lists available at ScienceDirect

Energy Conversion and Management: X

journal homepage: www.sciencedirect.com/journal/energy-conversion-and-management-x

A techno-economic and life cycle assessment of a new power and biomass to liquids (PBtL) configuration with negative emissions for producing sustainable aviation fuel (SAF)

Maria Fernanda Rojas-Michaga [a,*], Stavros Michailos [b], Evelyn Cardozo [c], Kevin J. Hughes [a], Derek Ingham [a], Mohamed Pourkashanian [a]

[a] Energy 2050, School of Mechanical, Aerospace and Civil Engineering, The University of Sheffield, Sheffield, S3 7RD, United Kingdom
[b] School of Engineering, University of Hull, Hull HU6 7RX, United Kingdom
[c] Centro Universitario de Investigaciones en Energías, Facultad de Ciencias y Tecnología, Universidad Mayor de San Simón, Bolivia

ARTICLE INFO

Keywords:
Biomass gasification
Fischer-Tropsch
Power-and-Biomass-to-Liquids
Bioenergy with Carbon Capture and Storage
Techno-economic assessment
Life cycle assessment

ABSTRACT

A novel configuration of the hybrid Power-and-Biomass to Liquids (PBtL) pathway for producing sustainable aviation fuels (SAF) has been developed and assessed from a techno-economic and environmental perspective. The proposed configuration can achieve negative emissions and hence a new bioenergy with carbon capture and storage (BECCS) route is proposed.

The amount of CO_2 that is captured within the process and that is sent for storage ranges from 0 % to 100 %, defining the various PBtL-CCS scenarios that are evaluated. Mass and energy balances have been established through process modelling in Aspen Plus and validated using data available in the literature. Further, the System Advisor Model (SAM) tool was used to model a dedicated offshore wind farm, based on location specific wind data. Results from the technical assessment have set the foundation for economic and environmental evaluations. The economic evaluation of the proposed SAF production configurations estimates minimum jet fuel selling prices (MJSP) ranging from 0.0651 to 0.0673 £/MJ, mainly driven by electricity consumption and feedstock cost. Costs for CO_2 compression, transport, and storage have a small contribution to the MJSPs of all the proposed scenarios. Global warming potentials range from −105.33 to 13.93 gCO_{2eq}/MJ, with PBtL-CCS scenarios offering negative emissions and aligning with the aviation industry's net-zero ambition for 2050. Water footprints range from 0.52 to 0.40 l/MJ, mainly driven by the water requirements of the alkaline electrolyser and refinery, followed by the wind electricity water footprint. Based on the outputs of the assessments, the resulting SAF could benefit of the support proposed by the UK SAF mandate, which could boost their economic performance by awarding certificates with monetary value. Estimates indicate that the cost of certificates that breakeven the fossil jet fuel price could reduce if negative emissions are also rewarded under this scheme.

Abbreviations: AACE, Association for the Advancement of Cost Engineering; AC, Alternating Current; AE, Alkaline Electrolyser; ASU, Air Separation Unit; BECCS, Bioenergy carbon capture and storage; BtL, Biomass-to-Liquid; C, Compressor; CAPEX, Capital Expenditures; CCS, Carbon Capture and Storage; CDR, Carbon Dioxide Removal; CEPCI, Chemical Engineering Plant Cost Index; DAC, Direct Air Capture; DC, Direct Current; DC1, Distillation Column; DCFA, Discounted Cash Flow Analysis; DFBG, Dual Fluidised Bed Gasifier; FCI, Fixed Capital Investment; FOM, Fixed operating and maintenance costs; FR, Forest residues; FT, Fischer-Tropsch; GHG, Green-House-Gas; GLS, Gas-Liquid Separator; GLLS, Gas-Liquid-Liquid Separator; GWP, Global Warming Potential; HDCR, Hydrocracking Reactor; HP, High Pressure; HR, Hydrogenation Reactor; HX, Heat Exchanger; IC, Indirect Cost; IDC, Installed direct costs; ISO, International Organization for Standardization; KPI, Key performance indicator; LCA, Life Cycle Assessment; LCI, Life Cycle Inventory; LCOE, Levelised cost of Electricity; LHV, Low Heating Value; LP, Low Pressure; MJel, Megajoules of electricity; MJSP, Minimum Jet Fuel Selling Price; MJth, Megajoules of thermal energy; MM, Millions; MP, Medium Pressure; NIDC, Non-installed direct costs; NPC, Net Present Cost; NPV, Net Present Value; NREL, National Renewable Energy Laboratory; OPEX, Operating Expenses; P, Pump; PBtL, Power-and-Biomass to liquids; PEC, Purchase Equipment Cost; PtL, Power-to-Liquids; RED II, Renewable Energy Directive II; RFS, Renewable Fuels Standard; RoW, Rest of the World; RWGS, Reverse Water Gas Shift; SAF, Sustainable aviation Fuel; SAM, System Advisor Model; T&S, Transport and storage; TCR, Total Capital Requirement; TDC, Total Direct Costs; TEA, Techno-economic assessment; TRL, Technology Readiness Level; UNFCC, United Nations Framework Convention on Climate Change; VC, Variable Operating Costs; WC, Working Capital; WGS, Water Gas Shift; WtWa, Well-to-Wake; W, Work (power); WW, Waste Water.

* Corresponding author.
E-mail address: m.rojasmichaga@sheffield.ac.uk (M.F. Rojas-Michaga).

https://doi.org/10.1016/j.ecmx.2024.100841
Received 9 October 2024; Received in revised form 12 December 2024; Accepted 15 December 2024
Available online 16 December 2024

Overall, the study introduces for the first time and assesses a novel net-negative SAF configuration, and the new information generated provides meaningful insights to a variety of stakeholders such as process developers, academics and policy makers.

Nomenclature

C	Carbon
CI_{factor}	Carbon intensity factor (gCO_{2eq}/MJ)
CI_{SAF}	Carbon intensity of the SAF (gCO_{2eq}/MJ)
CI_F	Carbon intensity of the fossil jet fuel (gCO_{2eq}/MJ)
CO_2	Carbon dioxide
gCO_{2eq}	Grams of CO_2 equivalent
H	Hydrogen
LHV_{fuel}	Low heating value of the fuel (MJ/kg)
LHV_{SAF}	Low heating value of SAF (MJ/kg)
$\dot{m}_{fuels}$	Mass flow of the fuel (kg/s)
m_{SAF}	Mass of the SAF (kg)
η_C	Carbon efficiency
$\dot{n}_{C,\ hydrocarbons}$	Molar flow of carbon content in hydrocarbons (mole C/h)
$\dot{n}_{C,\ feedstock}$	Molar flow of carbon content in biomass (mole C/h)
η_H	Hydrogen efficiency
$\dot{n}_{H,\ hydrocarbons}$	Molar flow of hydrogen content in hydrocarbons (mole H/h)
$\dot{n}_{H,\ feedstock}$	Molar flow of hydrogen content in biomass (mole H/h)
η_{PBtL}	PBtL efficiency
P_{DAC}	DAC unit's power demand (MW)
P_{El}	Electrolyser's power demand (MW)
$P_{process}$	Process' power demand (MW)

Introduction

Background

Growing concerns about global warming and the significant contribution of the aviation industry to anthropogenic emissions (2 % in 2019) [1] have intensified efforts to decarbonize the sector. While electrification holds long-term promise, the near-term focus is on developing and implementing sustainable aviation fuels (SAF). [2]. Achieving significant greenhouse gas (GHG) emissions reductions requires widespread SAF adoption. To meet the ambitious net-zero emissions target of the aviation industry by 2050 [3] a diverse range of production technologies is essential. Currently, no SAF production pathway is able to deliver 100 % emissions reduction. As a result, net-zero emissions could only be achieved by developing or introducing carbon dioxide removal (CDR) technologies such as bioenergy with carbon capture and storage (BECCS) and/or carbon offsets [3,4]. The former solution is a more efficient and transparent solution to offset residual emissions and hence combining BECCS to SAF production technologies leads to fuels with negative emissions, and this concept could be benefited from higher subsidies while supporting the net-zero development goal of the aviation industry [5].

Biomass to Liquid (BtL) SAF production technologies require careful feedstock selection, since life cycle assessment (LCA) studies have demonstrated that, due to land use change, some biofuels could have higher GWP compared to fossil jet fuel [6]. Further, the availability of significant amounts of sustainable and high-quality biomass may limit the production of SAF in regions lacking this resource. The Power-to-Liquids (PtL) pathway, on the other hand, is promising in terms of scalability, but its deployment is still restricted by the early stage of development of some of its constituent technologies. Moreover, compared to other SAF production technologies, the PtL configurations have large electricity requirements, low energy efficiencies, and high production costs [1,5]. Despite all these limitations, meeting the demand of the 2050 SAF market will require the use of both BtL and PtL technologies [1].

Several TEA and LCA assessments of BtL scenarios are found in the literature, while fewer studies have been conducted on PtL scenarios for the production of SAF. For instance, BtL scenarios for SAF production have demonstrated that significant reductions in greenhouse gas emissions can be achieved compared to conventional jet fuels [6–9]. The efficiency of these scenarios varies depending on the configuration and process optimization, with key challenges such as biomass availability, which have a major impact on both economic and environmental performance [10–12]. On the other hand, studies related to PtL for SAF production have found that PtL has more advantages over BtL, as it is not restricted by feedstock availability. Another advantage is the potential for near-zero emissions [13,14], depending on the energy source used. However, PtL scenarios tend to be more expensive due to the high-energy demand [14–18].

The PBtL is a hybrid configuration that combines the original BtL and PtL technologies while also producing drop-in SAF. This process is performed through various integrated stages, including water electrolysis, biomass gasification, and liquid fuel synthesis and separation units. The synthesis of hydrocarbons typically occurs in a Fischer-Tropsch (FT) reactor; prior to FT, syngas production step is achieved via biomass gasification, the reverse water gas shift (RWGS) reactor, or by the direct injection of H_2 [19,20]. Several studies that evaluated the FT- PBtL technology exist in the literature [19–33], and configurations integrating nuclear energy [34] or ethanol and electricity to SAF [35] have been also proposed. A summary of the technical findings indicates that the PBtL process enhances the BtL carbon conversion efficiency, therefore increasing fuel productivity. Moreover, when compared to the PtL configuration, the PBtL scenario requires less energy per unit of fuel, therefore achieving higher energy efficiency.

Hillestad et al. [21] found PBtL diesel more profitable than BtL diesel. However, Dietrich et al. [19] reported lower NPC for BtL liquid fuels compared to PBtL and PtL. While extensive techno-economic assessments (TEAs) exist for BtL and PtL SAF, studies on PBtL SAF are limited [20,29]. Habermeyer et al. [30] evaluated a PBtL small-scale experimental facility for FT fuel production with an integrated TEA and LCA approach. The conceptual design of this facility includes a water scrubber for the separation of the CO_2 from the syngas, which is further recycled to the gasifier to substitute the steam as gasification medium. This setup eliminated the need for a RWGS reactor, resulting in H_2 injection occurring prior to the FT reactor, but downstream purification and separation units were excluded from the assessment. The resulting NPC of the PBtL C_{5+} hydrocarbons was estimated at 0.029 $£_{2020}$/MJ [30], while for a large-scale plant, the same authors estimated a NPC equal to 0.036 $£_{2020}$/MJ [20].

Limited LCA studies exist for PBtL configurations [20,29,30,32] primarily focusing on global warming potential (GWP) impact. These studies concluded that the major contributor to the GWP is the consumed electricity. When compared to analogous BtL or PtL scenarios,

the GWP of the PBtL process was lower or higher, [30,32] depending on the energy source that was used. Habermeyer et al. [20,30] performed the only SAF-oriented LCA; the boundaries of this LCA did not include the post-FT separation processes and hence it was a well-to-refinery gate assessment. Their results briefly explored several environmental impacts in addition to the GWP; the latter resulted in a positive value regardless of the source of electricity used. However, due to the missing separation section, the estimated environmental impacts would be different to a WtWa scenario since the various hydrocarbon fractions that are produced in the process plant imply the presence of a multifunctional system.

Previous studies have explored the feasibility of PBtL, but none have achieved negative emissions. Recent research, such as that by Habermeyer et al. [20,30], demonstrates that significant emission reductions relative to conventional aviation fuel are possible, though no configuration has yet achieved negative emissions. Given the growing interest in Carbon Dioxide Removal (CDR) technologies as a strategy to limit global warming to 1.5 °C [36], particularly within the aviation sector aiming for net-zero emissions by 2050, there is a need to explore BtL-CCS configurations further. While some studies exist on SAF from BtL-CCS [37,38], none has evaluated the PBtL-CCS configuration, which, if properly designed, could produce pure CO_2 streams for storage, creating potential for negative emissions.

Research gaps and novelties

This study makes several novel contributions to the field of SAF production. First, it proposes for the first time a new process design that can produce SAF and achieve negatives emissions. To holistically assess the proposed PBtL-CCS configuration, we have employed exhaustive technical process modelling, TEA, WtWa LCA and existing policy schemes studies.

The focus of the study is to design new configurations capable of achieving negative emissions, and hence to contribute to the aviation industry's efforts to offset residual emissions. Furthermore, the research assesses the potential impact of monetary policy schemes, i.e. the UK SAF mandate, on the viability of the project. In addition, sensitivity and probabilistic assessments are performed to evaluate the level of uncertainty in the estimated economic and environmental indicators.

The following research questions guide this study:

1. Can the PBtL-CCS configuration for SAF production achieve negative emissions, and if so, under what conditions?
2. What are the key economic and environmental performance indicators for the PBtL-CCS process, and how do they interact under a Well-to-Wake (WtWa) scenario?
3. How do uncertainties in economic and environmental assessments influence the viability of SAF production via the PBtL-CCS configuration?
4. What impact does the UK's preliminary SAF mandate have on the economic feasibility and environmental sustainability of these pathways?

Goal and scope of the study

The primary goal of this research is to propose a SAF configurations that can achieve negative emissions and hence contribute to the deep decarbonisation of the aviation industry and offset residual emissions. The results of the current study can provide meaningful information to conceptual engineering studies, academics and policy makers. The objectives can be summarised as follows:

- To design a Power-Bio-to-Liquid with Carbon Capture and Storage (PBtL-CCS) process.
- To establish mass and energy balances through process modelling.
- To assess the technical, economic, and environmental performance of the investigated routes.
- To carry out a sensitivity analysis and identify the parameters with the greatest impact on the economic and environmental indicators.
- To assess the effect of the UK SAF mandate on the viability of the SAF routes.

Methods

This section details the methodology for evaluating the proposed PBtL-CCS configurations. It covers plant capacity and location selection, Aspen Plus modelling (with additional details in the supplementary materials), and techno-economic and environmental analysis.

Capacity and location of the plant

The production of SAF from biogenic residues that are not detrimental to normal food provision and/or constitute a danger of deforestation are supported by the UK SAF mandate [39]. Given the availability in the UK, forest residues (FR) are selected as the source of carbon for the proposed system. A processing capacity of 20 dry-tonnes per hour of FR is considered, as proposed in a previous study by the authors [37]. This capacity is below the estimated UK availability of FR for biofuel production [40]. Furthermore, even in the most pessimistic regional availability scenario, this plant capacity would ensure sufficient FR for other uses beyond SAF production [39].

The operation of PBtL configurations depends on a large supply of low carbon electricity [41]. The UK has a great potential for offshore wind electricity generation, and the UK government has recently declared the goal of achieving an installation capacity of up to 50GW of offshore wind by 2030 [42]. A dedicated off-shore wind farm is integrated into the proposed PBtL-CCS scenarios. The SAF production plant is located in the Humber area (Teeside), due to its optimal wind profile, and its proximity to Scotland, which contains most forests of public ownership [40] This aligns with the decarbonisation goals of the East Coast Cluster, encompassing Teesside and Humber [43]. The Endurance Reservoir, a North Sea saline aquifer 145 km offshore, is a potential primary CO_2 storage site, as proposed by the cluster [44].

System description and modelling

This section outlines the key assumptions and specifications used to model the scenarios. It begins with a high-level overview of the system, including brief descriptions of its key process units and their mass and energy interactions. Subsequent sections thoroughly explain these processes and how they are represented in Aspen Plus. Additional sections describe the methodology for heat integration and wind farm sizing. Finally, the key performance indicators are defined.

System description

Fig. 1 depicts the main components of the process configuration:

1. Pre-treatment: Forest residue chips are ground and dried.
2. Gasification: Syngas is produced from the thermal treatment of the pre-treated forest residues.
3. Syngas cleaning: This section includes the ash separator, the tar reformer and the zinc oxide bed for the separation of the sulphur.
4. Syngas Upgrading: Cleaned syngas, along with recycled CO_2, and hydrogen is fed to the RWGS to increase the yield of the syngas.
5. Hydrocarbon synthesis and separation: Syngas is converted to syncrude in the FT reactor. The syncrude is separated into naphtha, kerosene, diesel, and wax. Wax is hydrocracked to produce smaller hydrocarbons.
6. CO_2 capture and storage: CO_2 from the gasifier and unreacted syngas is captured. Part of the CO_2 is recycled to the RWGS reactor, while the rest is sent for compression. This section takes the gaseous CO_2 to

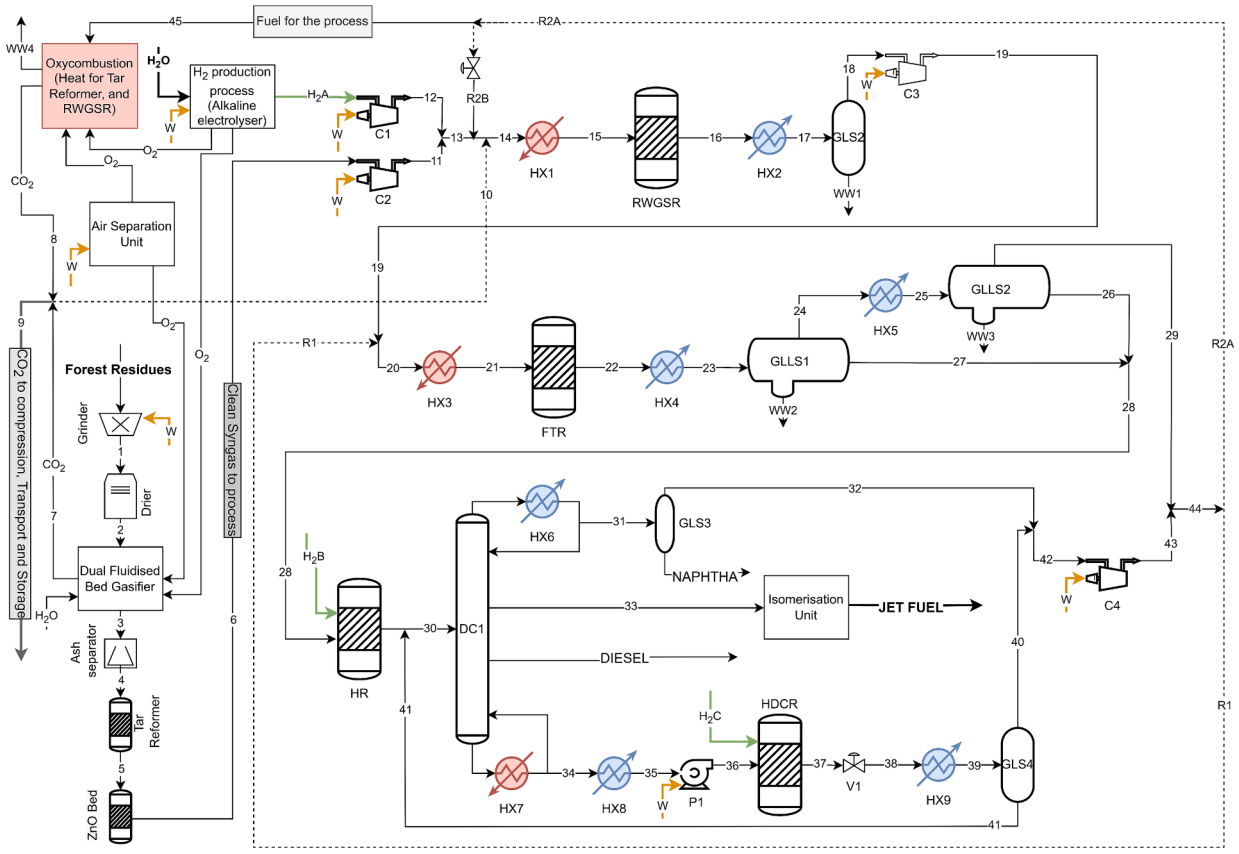

Fig. 1. Flowsheet of the PBtL scenarios for SAF production (process plant boundaries).

supercritical conditions, enabling its subsequent transport and storage [45,46]. Seven scenarios with varying CO_2 storage percentages (0–100 %) are analysed, as presented in Table 1. A purge stream is included in the 0 % storage scenario to prevent gas build-up [47].

7. Hydrogen and oxygen production: An alkaline electrolyser produces hydrogen for various process units. The by-product oxygen is used for oxycombustion, providing high-temperature heat to the RWGS and tar reformer, and is also used in the combustion chamber of the gasifier. In cases where the oxygen generated by the electrolyser is below the requirement, an air separation unit (ASU) is added to the process to support the oxygen supply.

Table 1
Description of the investigated scenarios.

Scenario name	Description	Type of process configuration
0 %TS	0 % of the total CO_2 stream is sent for storage. 2 % of the total CO_2 stream is purged.	PBtL
20 %TS	20 % of the total CO_2 stream is sent for storage.	PBtL-CCS
40 %TS	40 % of the total CO_2 stream is sent for storage.	PBtL-CCS
50 %TS	50 % of the total CO_2 stream is sent for storage.	PBtL-CCS
60 %TS	60 % of the total CO_2 stream is sent for storage.	PBtL-CCS
80 %TS	80 % of the total CO_2 stream is sent for storage.	PBtL-CCS
100 %TS	100 % of the total CO_2 stream is sent for storage.	PBtL-CCS

TS: Transport and Storage.
PBtL: Power-and-Biomass to liquids.
PBtL-CCS: Power-and-Biomass to liquids with Carbon Capture and Storage.

Process modelling

Aspen Plus V14 is used to model the refinery plant, excluding the ASU and the alkaline electrolyser, whose mass and energy balances are taken from Holst et al. [48] and Young et al. [49], respectively. The RKS-BM method is selected for the representation of the thermodynamic and physical–chemical property calculations, suitable for hydrocarbon processing facilities [50]. Solid streams, such as biomass and ash, are treated as non-conventional solids without particle size distribution [37].]. Table 2 presents ultimate and proximate composition of FR. Detailed descriptions of the refinery sections depicted in Fig. 1 can be found in Section S.1 of the Supplementary Materials. For more information on the equipment, readers are invited to refer to previous studies by the authors [14,37].

Off-shore wind farm

The system is coupled to a dedicated offshore wind farm, as proposed in a previous study [14]. Hourly wind speed data from NASA-MERRA 2

Table 2
Proximate and ultimate analysis of forest residues [51].

Proximate analysis (%)	Forest residues
Moisture (as received)	30
Fixed carbon (dry basis)	17.16
Volatile matter (dry basis)	82.29
Ash (dry basis)	0.55
Ultimate analysis (mass %)	
Carbon	50.54
Hydrogen	7.08
Nitrogen	0.15
Sulphur	0.57
Oxygen	41.11
Ash	0.55

[52], for Teeside (Fig. 2) is used to estimate power generation. The wind speeds are given at a height of 10 m; however, they are adjusted to 80 m as required by the software System Advisor Model (SAM) [53]. Given that the hourly wind speed fluctuates, the power production will have the same behaviour. Constant power supply to the electrolyser could prolonged its lifespan [54]. To ensure consistent power supply to the electrolyser, the system interfaces with the grid, storing excess energy and drawing power as needed that is used for calculating the power generation curve [55,56]. The number of turbines is optimised to balance annual energy input and output [56]. Other alternatives such as the annexation of a battery bank [55,57–59] was not analysed, since it has been found to have high capital cost and low energy efficiency [55,56]. More details on the design of the wind farm can be found in [60].

Technical performance indicators

To compare the technical performance of the studied scenarios with each other and with analogous BtL [37], and PtL [60] processes, the carbon conversion, hydrogen conversion and PBtL efficiencies are estimated based on Equations (1), 2, and 3, respectively.

$$\eta_C = \frac{\dot{n}_{C,\ hydrocarbons}}{\dot{n}_{C,\ feedstock}} \tag{1}$$

$$\eta_H = \frac{\dot{n}_{H,\ hydrocarbons}}{\dot{n}_{H,\ feedstock}} \tag{2}$$

$$\eta_{PBtL} = \frac{\left|\dot{m}_{fuels} \bullet LHV_{fuel}\right|}{P_{El} + P_{DAC} + P_{process}} \tag{3}$$

Where $\dot{n}_C$ and $\dot{n}_H$ stand for carbon and hydrogen molar flows respectively, for either the hydrocarbon commercial fractions (naphtha, SAF, and diesel), or the feedstock (biomass, steam, hydrogen). $\dot{m}_{fuels}$ is equivalent to the mass flow of the hydrocarbons, and LHV_{fuel} is equivalent to the low heating value of them, being 42.6 MJ/kg [61], 44.9 MJ/kg [61] and 42.8 MJ/kg [62], for naphtha, diesel and kerosene respectively. For Forest residues, the calculated LHV based on a 30 % moisture content equals 12.95 MJ/kg assuming a dry basis LHV of 19.54 MJ/kg [63]. Finally P stands for the electricity consumption for the electrolyser, process plant and the ASU.

Economic assessment

The economic feasibility of the SAF production scenarios is reflected throughout the estimation of relevant KPIs, such as the CAPEX, OPEX and MJSP. These are calculated based on several assumptions as presented in Table 3, and by using discounted cash flow analysis (DCFA). The MJSP stands for the minimum selling price of the SAF at which the income and outcome are equal, and therefore the net present value (NPV) is zero [12,64,65]. The nth plant assumption is adopted, considering the relatively high maturity of most technologies.

Life cycle assessment

The environmental impact of the SAF production and utilisation was evaluated using a Well-to-Wake (WtWa) life cycle assessment (LCA). The standardised approach outlined in the standards ISO 14040 and 14,044 was adopted for consistency and transparency of the LCA [66]. The LCA is divided into four main stages: Goal and scope definition, life cycle inventory, impact assessment and interpretation [67]. The following sections will briefly explain the assumptions adopted for the assessment.

Goal and scope definition

The primary objective of this study is to quantify and compare the environmental impacts of SAF production through various PBtL-CCS

Table 3
Main adopted assumptions for the economic assessment [12,64,65].

Location	United Kingdom
Plant life	20 years
Currency	£
Base year	2022
Plant capacity (based on feedstock input)	20,000 kg FR/h
Discount rate	10 %
Tax rate	30 %
Construction period	3 years
First 12 months' expenditures	10 % of FCI
Next 12 months' expenditure	50 % of FCI
Last 12 months' expenditures	40 % of FCI
Depreciation method	Straight line
Depreciation period	10 years
Working capital	5 % of FCI
Start-up time	6 months

*FCI = Fixed Capital Investment.

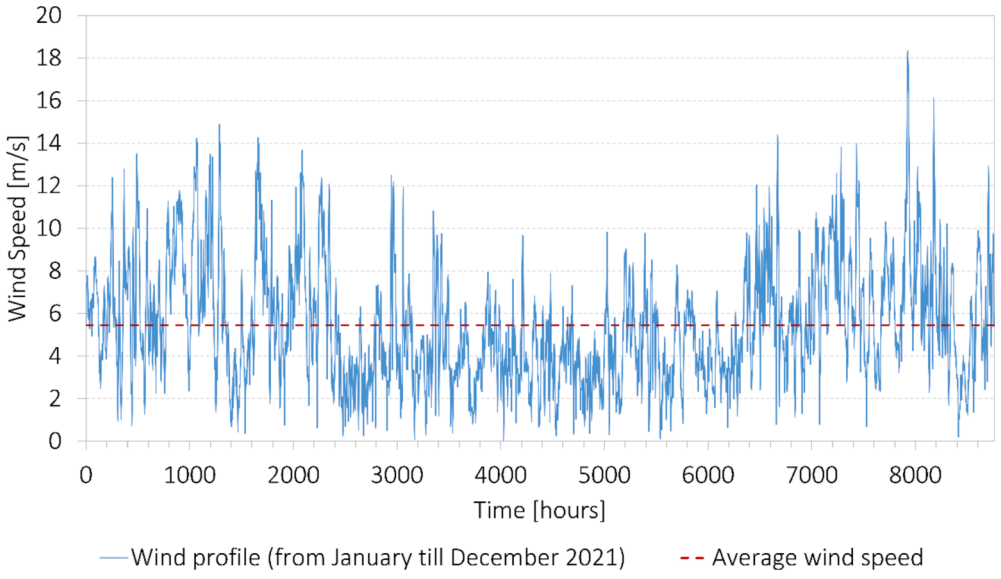

Fig. 2. Hourly wind profile for Teeside as extracted from the NASA MERRA 2 database [60].

scenarios with conventional jet fuel. The analysed scenarios share a common process configuration but vary in the amount of CO_2 captured and stored (0 %, 20 %, 40 %, 60 %, 80 %, and 100 %). The system boundary extends from resource extraction and raw material production to SAF utilization (combustion or end-of-life), constituting a WtWa assessment, as illustrated in Fig. 3. The functional unit is defined as 1MJ of SAF produced, based on its LHV of 42.8 MJ/kg [62]. The geographical scope of this assessment is the UK.

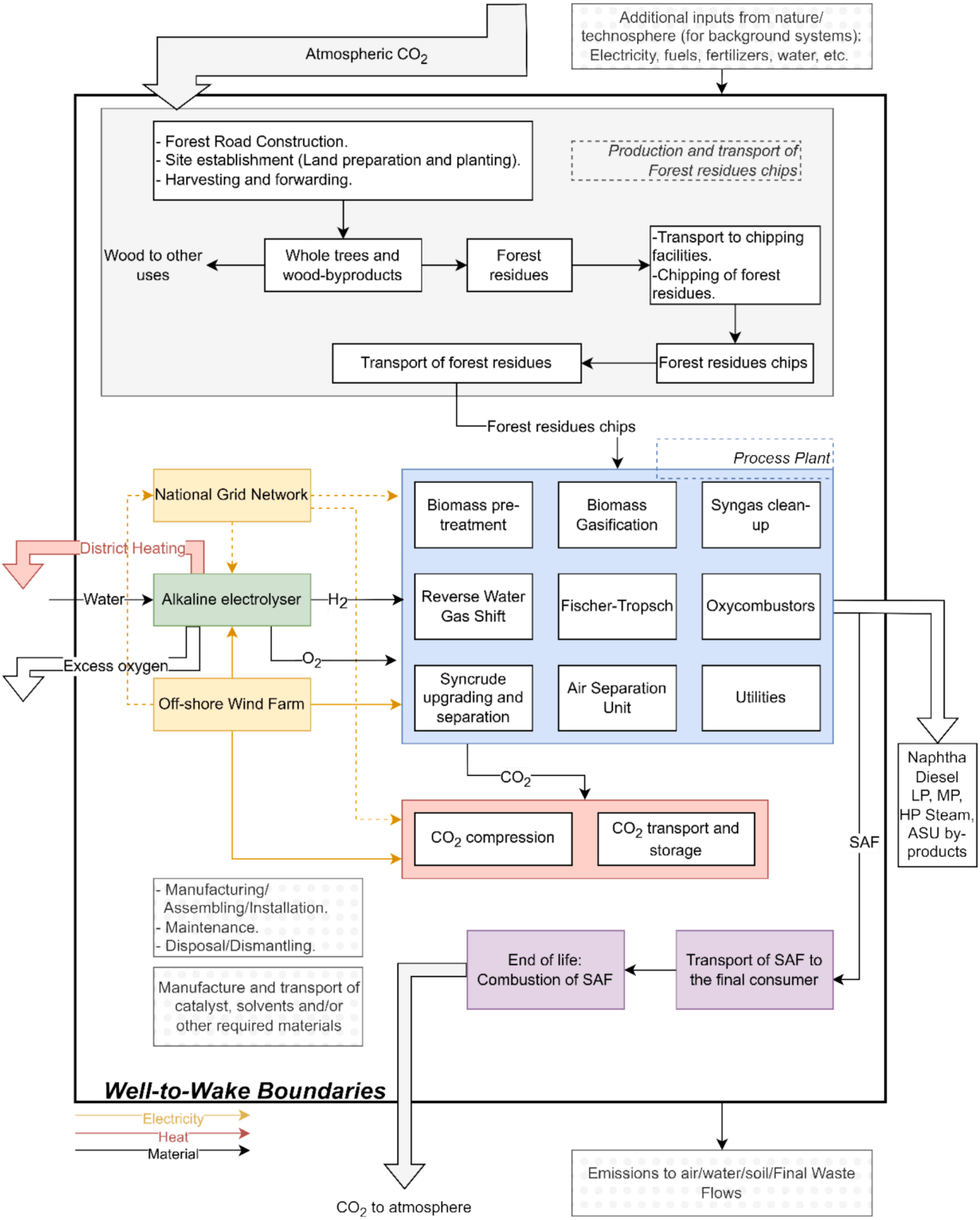

Fig. 3. Well-to-Wake boundaries of the life cycle assessment of the PBtL-CCS scenarios.

Life cycle inventories

This section details the data collection for mass and energy flows within the LCA and its interactions with the environment. Data sources are categorised as foreground and background. The foreground LCI is primarily based on mass and energy balances from Aspen Plus models. The Ecoinvent 3.6 database, along with other external sources, is used for background LCI and to supplement missing foreground LCI data. The comprehensive database of Ecoinvent offers a wide range of LCI data for various sectors. The "allocation, cut-off by classification-system" approach, recommended by Ecoinvent [68] is used for system modelling. Given the chosen location for the SAF production plant, preferably, UK LCI data are prioritised. If unavailable, European, Global, or Rest of the World databases are selected, in descending order of preference. More insight on the assumptions and data sources of the LCI for the stages inside the system's boundaries is provided in section S.3 of the Supplementary Materials.

Multi-functionality

ISO 14040 guidelines initially advise addressing a multifunctional system through system expansion. However, when this approach is not applicable, physical allocation or economic allocation are suggested [69]. Past LCA studies on sustainable fuel production have shown that system expansion often underestimates the overall environmental impact of a system, especially when co-products displace high-emission goods, such as those originated from fossil fuels [6,37,70]. In this sense, energy allocation is preferred for such systems and is adopted in this study.

The boundaries of the proposed SAF production process contain two multifunctional systems: The alkaline electrolyser (AE) and the refinery plant. Allocation in this context refers to the distribution of environmental impacts related with the operation and maintenance of the system, as well as the upstream environmental impacts of all inputs (energy, or materials), among the various outputs of the system. Table 4 describes the baseline allocation approach and additional complementary approaches.

The "baseline approach" is a conservative allocation method recommended by a methodological tool by the UNFCC [71], where emissions are allocated only to the main products. For the alkaline electrolyser AE, this means all emissions from electrolysis and upstream activities are attributed solely to hydrogen production [72]. Similarly, in the refinery plant, emissions are allocated to the main fuels (SAF, diesel, and naphtha) on an energy basis, assuming by-products are produced in small quantities or have limited economic or energy significance compared to main products [71,73].

In the baseline approach, CO_2 storage benefits are allocated solely to the primary product, SAF, as it is the focus of the environmental assessment. Here, the negative emissions from CO_2 storage reduce only the Well-to-Wake (WtW) GWP of SAF. Intuitively, this baseline scenario should result in a more negative GWP for SAF. In contrast, in Approach 1b, CO_2 storage benefits are divided among SAF, naphtha, and diesel based on their energy content. Therefore, the share of the CO_2 negative emissions for the SAF is deducted from the WtW GWP of SAF to find the final GWP. To provide a broader perspective, additional allocation approaches are explored in Table 4, and their results are discussed in the sensitivity analysis.

Impact assessment

For the evaluation of the environmental impact as described in the LCIs of the different stages of the system, the ReCiPe midpoint (H) method was chosen. This method is widely applied by LCA practitioners, as it calculates 18 midpoint impact categories, among which the GWP100 [74]. The accounting of the carbon requires a differentiation between the one of biogenic or fossil origin due to the storage of CO_2. Biogenic feedstock, such as forest residues requires an uptake of atmospheric CO_2, which is listed as "Carbon dioxide, in air" in the "Inputs from nature" section of the wood chips LCI from Ecoinvent. This carbon experiences a series of physical and chemical transformation until it is released back to the air during the combustion of the SAF; therefore, null GWP characterization factors are assigned to the "Carbon dioxide, in air" and "Carbon dioxide, biogenic" as suggested by the IPCC guidelines [75]. However, not all captured carbon is released during combustion, as some scenarios involve CO2 storage. In such cases, biogenic CO2 storage is considered a "negative emission" [76], and a characterization factor of "-1" is applied.

Sensitivity and uncertainty analysis

Tables 5 and 6 summarize the parameters identified as having the greatest uncertainty, which, according to previous studies [37,60], are also the primary contributors to the final economic and environmental performance indicators.

The uncertainty range of −30 % to + 50 % for the process plant's CAPEX is based on AACE International recommendations [77]. To simplify analysis, the H_2 production cost is varied instead of individually analysing the uncertain CAPEX and OPEX of the AE. Minimum and maximum discount rates and tax rates represent optimistic and pessimistic scenarios, respectively [78]. Additionally, an optimistic scenario assumes exemption on grid electricity network cost payments for renewable projects [79]. A ± 50 % uncertainty range is applied to other parameters. A separate scenario, not included in the probabilistic TEA, considers the sale of naphtha and diesel at the same price as SAF.

Five key parameters were selected for the sensitivity analysis of GWP, as shown in Table 6. Previous studies have highlighted the significant impact of electricity source on PBtL and PtL configurations.

Table 4
Allocation approaches for the multifunctional system of the WtWa PBtL system.

System	Product/co-product/ by-product	Approach 1 (baseline allocation approach)	Approach 1b	Approach 2	Approach 3	Approach 4
Alkaline Electrolyser	Allocation	no*	no*	Yes, exergy	no*	no*
	Hydrogen	yes	yes	yes	yes	yes
	Oxygen	no	no	yes	no	no
	District heating	no	no	yes	no	no
Refinery Plant and upstream inputs	Allocation	Yes, energy	Yes, energy	Yes, energy	Yes, exergy	Yes, economic
	SAF	yes	yes	yes	yes	yes
	Naphtha	yes	yes	yes	yes	yes
	Diesel	yes	yes	yes	yes	yes
	LP,MP,HP Steam	no	no	no	yes	yes
	By-products from ASU	no	no	no	yes	yes
CO_2 storage benefits (negative emissions)	Allocation	Only to SAF**	Divided between SAF, naphtha and diesel on an energy basis	Only to SAF**	Only to SAF**	Only to SAF**

*Meaning that no allocation is applied, and all the emissions go to the produced hydrogen.
**Meaning that the total net negative emissions generated in the CO_2 storage are deducted from the WtWa GWP of the SAF.

Table 5
Parameters included in the sensitivity and uncertainty analysis of the TEA.

Parameter	Nominal value (for all the scenarios)	Minimum	Maximum
H_2 generation cost [£/kg H_2]	*Different for each scenario (to be presented in results section)	1	8
CAPEX refinery [MM£]		−30 %[a]	+50 %[b]
Cost of wind farm electricity [£/kWh]	0.06	−50 %[a]	+50 %[b]
Network cost [£/kWh]	0.01	0	–
TAX rate [%]	30	0	40
Discount rate [%]	10	8	12
Feedstock cost [£/kg]	0.06	−50 %[a]	+50 %[b]
If Naphtha and diesel gate prices same as MJSP of SAF	N/A	–	–

[a] Percentage points lower than the nominal value.
[b] Percentage points larger than the nominal value.

Table 6
Parameters included in the sensitivity and uncertainty analysis of the GWP.

Parameter	Nominal value (for all the scenarios)	Minimum	Maximum
Wind electricity carbon intensity [gCO_{2eq}/kWh]	15.25	7	22.5
GWP of FR chips production [gCO_{2eq}/kg wood chips dry basis]	42.35	−30 %[b]	+30 %[c]
GWP of Transport of FR chips [gCO_{2eq}/kg wood chips dry basis]	18.16	−30 %[b]	+200 %[c]
GWP of CO_2 compression, T & S [gCO_{2eq}/kg of CO_2 to storage]	3.22[a]	−10 %[b]	+10 %[c]
Alkaline Stack efficiency (%)	68.81	58.00	73.00
UK grid [gCO_{2eq}/kWh]	193.38	–	–
No upstream emissions wind electricity [gCO_{2eq}/kWh]	0	–	–
Allocation, Approach 2	–	–	–
Allocation, Approach 3	–	–	–
Allocation, Approach 4	–	–	–

[a] For the scenario 0 %TS, the nominal value of this parameter is 0.
[b] Percentage points lower than the nominal value.
[c] Percentage points larger than the nominal value.

Therefore, the GWP of wind farm electricity was tested, using a bandwidth based on a National Renewable Energy Laboratory (NREL) report [80] that summarised and harmonised the findings of numerous LCA studies. The AE efficiency range was determined from literature values [81–84]. For the GWP of FR production and transport, and CO_2 compression, ±30 % or ± 10 % uncertainty ranges were applied, depending on their uncertainty level [37]. A maximum + 200 % range was set for FR transport to account for potential long-distance feedstock sourcing. Additionally, the impact of different allocation methods, as outlined in Table 4, was assessed.

Probabilistic TEA and LCA are important for capturing the uncertainty inherent in estimating parameters [85]. This study employed a Monte Carlo simulation approach to assess the impact of uncertain parameters listed in Tables 5 and 6. A triangular distribution was assumed for all parameters, and 10,000 trials were conducted. In each trial, uncertain parameters were randomly sampled within their defined ranges. The resulting MJSP and GWP values were used to calculate mean, median, and standard deviation estimates.

Limitations of the study

The new PBtL-CCS process presented herein is indeed a promising pathway for the production of SAF, nevertheless limitations still exist. Similar to any new technological process, the transition from theoretical and numerical results to real-world implementation involves several challenges and considerations. The integration of biomass gasification and hydrogen from electrolysis (especially when using renewable energy sources) aligns well with current sustainability goals. However, scaling this process to an industrial level involves addressing factors such as appropriate pilot design and testing, the availability of consistent biomass feedstock, the efficiency and cost of hydrogen production, the integration of these processes into existing industrial infrastructures, and the integration of the plant to a transport system for the captured CO_2. Further, this study focuses on the techno-economic and environmental implications of SAF production, a comprehensive assessment of fuel properties and their impact on aviation performance is also important. This type of assessment can provide valuable understanding of fuel compatibility, engine efficiency, emissions, and fuel handling, ensuring the safe and efficient operation of aircraft using new SAFs.

Furthermore, captured CO_2 offers a range of potential applications beyond storage, expanding the utility of the proposed configurations. While this has not been investigated, it could lead to different scenarios with different environmental and economic performance, especially considering the potential sale of captured CO_2 for various commercial and industrial uses. For instance, CO_2 serves as a feedstock for producing chemicals like methanol, urea, and polycarbonates [86]. It also finds applications in agriculture [87], food production [88], and the petroleum industry (for Enhanced Oil Recovery) [89].

Results

This section presents the results of the mass and energy balances, economic assessments, environmental impact assessments (including GWP and water footprint), and uncertainty analyses for different scenarios. Additionally, a brief policy assessment is provided to discuss the impact of the UK SAF mandate on the economic feasibility of PBtL-CCS SAF production.

Technical results

This section presents the results of the process models, including mass and energy balances. The material balances focus on carbon and hydrogen efficiencies to provide a clearer understanding of the proposed PBtL-CCS scenarios. Given the early stage of development of conceptual PBtL systems, there is no available data for validating the entire process plant. However, some functional units of the process are commonly found in oil-related plants, and these have been modelled based on recommendations from the literature. The Fischer-Tropsch section utilizes a model validated with experimental data by Marchese et al. [90]. The gasification composition was validated based on experimental results from a pilot plant using the specific type of gasifier, as detailed in the E4tech report [91].

Overall mass and energy balances, and PBtL efficiencies

Table 7 summarizes the key inputs and outputs from Aspen Plus simulations for each scenario. Given the energy-intensive nature of PBtL configurations, the electricity consumption breakdown for different process sections is also provided. While the forest residue input remains constant across scenarios, the amount of CO_2 sent for storage increases from 0 % to 100 % of the total CO_2 produced. This increased CO_2 storage leads to reduced carbon circulation within the refinery, lower SAF production, and decreased hydrogen demand (and consequently, lower electricity requirements). Notably, from the 50 %TS scenario onwards, reduced hydrogen demand requires the installation of an Air Separation Unit (ASU) to support the oxygen supply. The PBtL efficiency gradually improves with increasing CO_2 storage, primarily due to reduced electricity demand, particularly for the electrolyser, where a portion of the required electricity can be converted into heat.

Table 7
Main input/output process streams and electricity requirements for the proposed PBtL scenarios.

Main inlet/outlet streams [kg/h]	Scenario 0 %TS	20 %TS	40 %TS	50 %TS	60 %TS	80 %TS	100 %TS
Forest residues	28571.4	28571.4	28571.4	28571.4	28571.4	28571.4	28571.4
Naphtha	3294.35	2820.01	2493.33	2360.31	2221.73	2019.48	1830.23
SAF	6617.46	5770.66	4984.25	4668.55	4399.18	3909.27	3499.67
Diesel	1951.85	1707.36	1475.64	1382.95	1303.54	1158.97	1037.22
CO_2 to storage	658.69	5478.44	9514.38	11,185	12,688	15270.9	17494.1
Electricity requirements [MW]							
Electrolyser	286.41	219.68	164.73	142.49	122.98	89.13	61.22
Refinery plant	25.57	23.44	21.76	21.14	20.68	19.79	19.15
ASU	0	0	0	0.3	1.3	3.01	4.48
CO_2 compression	0	0.6	1.04	1.22	1.38	1.66	1.9
PBtL efficiency (%)	**34.05 %**	**35.44 %**	**36.85 %**	**37.55 %**	**38.09 %**	**39.31 %**	**40.41 %**
Carbon conversion efficiency (%)	**98.56 %**	**85.56 %**	**74.37 %**	**69.86 %**	**65.80 %**	**58.84 %**	**52.84 %**
Hydrogen conversion efficiency (%)	**21.52 %**	**21.84 %**	**22.07 %**	**22.19 %**	**22.27 %**	**22.49 %**	**22.59 %**

Electricity requirements, wind farm design and heat requirements

Table 7 details the electricity requirements for various process sections in the analysed scenarios. The electrolyser consistently demands the highest share of power, ranging from 71 % to 92 % of the total demand across all scenarios. The refinery plant follows, consuming between 8 % and 22 % of the total power. The remaining power is utilised by the ASU and/or CO_2 compression, depending on the specific scenario. Overall, the proposed scenarios are highly energy-intensive, primarily due to hydrogen production. Notably, the energy penalty associated with integrating CCS is minimal, even for scenarios with significant CO_2 storage.

To meet these considerable electricity requirements, a dedicated offshore wind farm was connected to the PBtL system, sized according to the criteria outlined in Section 2.5. Based on the wind speed profile and turbine model, the energy generation profile for each scenario was calculated using SAM software. Given the same wind profile and turbine model across scenarios, the energy generation profiles differ only in terms of total energy output. Consequently, only the 0 %TS scenario's profile is presented in Fig. 4. This profile highlights the variability in power supply, requiring a backup power system, particularly during spring and summer periods.

Table S.8 of theSupplementary Materials summarizes the number of wind turbines calculated for each scenario, the total power from the wind farm to the system, the power from the grid to the system, and the excess power from the wind farm to the grid. The estimated number of wind turbines decreases from 164 to 46 for the 0 %TS scenario to the 100 %TS scenario, as the electricity requirement gradually decreases. Moreover, there is a slight discrepancy between the excess wind electricity sent to the grid and the power received from the grid, but in all cases, the former is slightly larger than the latter.

Carbon and hydrogen conversion efficiencies

Figs. 5 and 6 illustrate the carbon and hydrogen flows through the refinery for various scenarios. Tables S.10 and S.11 provide quantitative details on molar flows. Carbon enters the system solely as forest residue and exits as gasoline, diesel, SAF, and CO_2. While the forest residue input remains constant, varying amounts of CO_2 are sent for storage, resulting in different carbon conversion efficiencies. The 0 %TS scenario has the highest efficiency, and the 100 %TS scenario the lowest (refer to Table 7).

Hydrogen enters the system through three sources: pure hydrogen from the AE, hydrogen contained in forest residues, and steam for gasification. It is either incorporated into fuels or lost as water during various reactions in the process. Consequently, the hydrogen conversion efficiency is constrained to values below 23 %, which is relatively low when compared to the estimated carbon conversion efficiencies. The amount of pure hydrogen required is directly linked to the available carbon, leading to similar hydrogen conversion efficiencies across

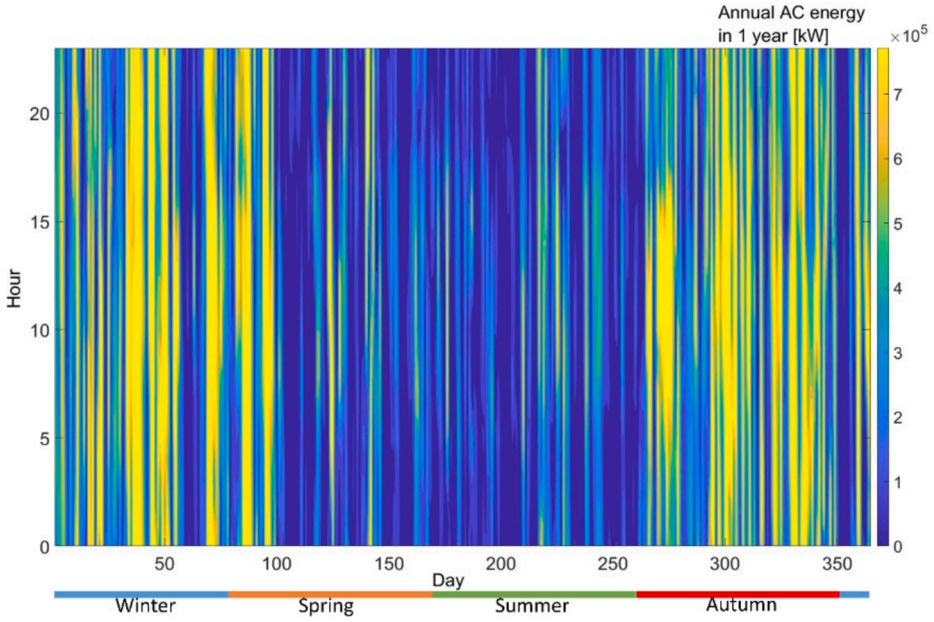

Fig. 4. Power curve for the wind farm of the 0 %TS scenario.

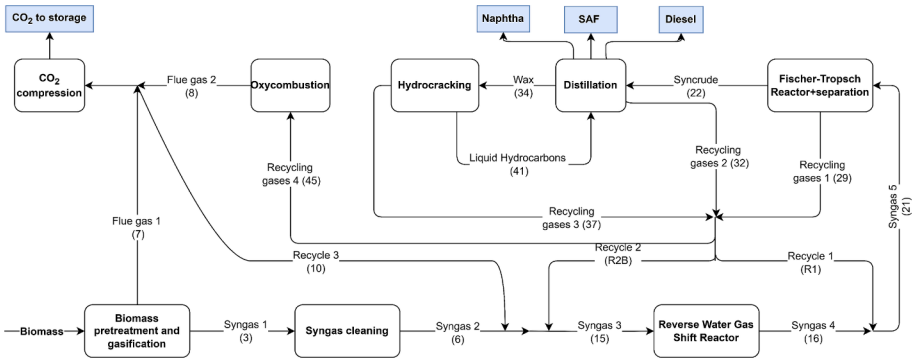

Fig. 5. Flow of carbon throughout the main process units of the refinery plant. (In parentheses, the stream names as labelled in Fig. 1).

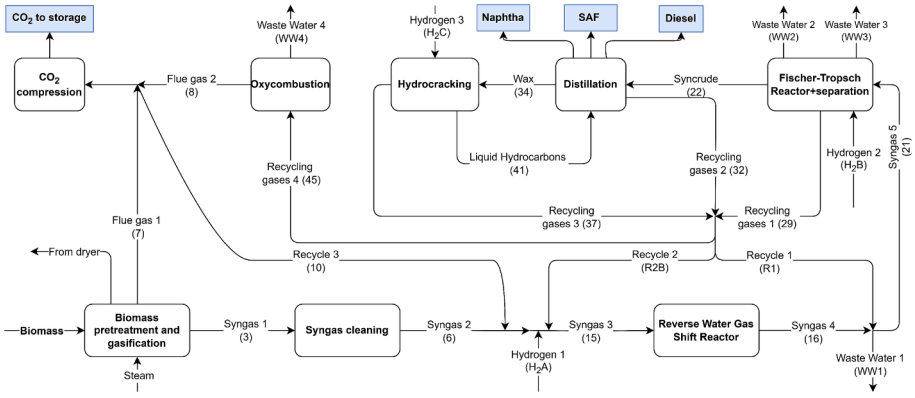

Fig. 6. Flow of hydrogen throughout the main process units of the refinery plant. (In parentheses, the stream names as labelled in Fig. 1).

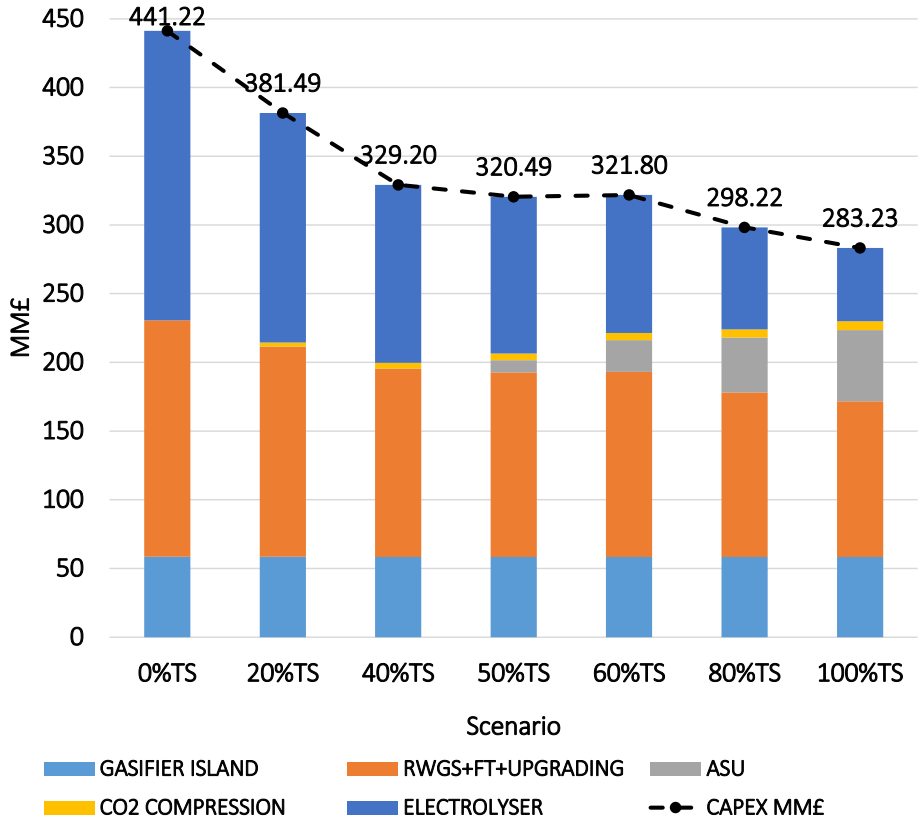

Fig. 7. CAPEX breakdown for the different scenarios.

scenarios, regardless of CO_2 storage levels.

A literature review reveals a variety of PBtL configurations for FT-syncrude production, differing in technologies and operating conditions, such as gasifier type, gasification agent, electrolyser type, and oxygen usage in fired heaters. Consequently, carbon conversion efficiencies reported in the literature range widely from 33.8 % to 97.7 %. Most studies indicate that PBtL processes offer higher carbon conversion efficiencies than BtL [19,21,25,30], and comparable or even lower efficiencies than PtL, depending on the configuration. In this study, the carbon conversion efficiencies of the PBtL scenarios, regardless of CO_2 storage levels, exceed those of an analogous BtL scenario [37]. The 0 %TS and 20 %TS PBtL scenarios achieve comparable carbon conversion efficiencies to a similar PtL system [60]. Further, in the literature, the reported PBtL efficiencies (32.1 % to 54.8 %) [19,30] align well with the calculated values (34.05 % to 40.41 %). While hydrogen conversion efficiency is not extensively discussed in PBtL literature, both PBtL and PtL configurations exhibit low efficiencies due to water production in FT and RWGS reactors.

Heat integration

The process models also estimate heating and cooling requirements, visualized as hot and cold composite curves in Section S.4. The absence of a pinch point temperature indicates a "threshold problem," requiring a single thermal utility. All scenarios are self-sufficient in terms of heat, requiring only external cold utilities. Post-heat integration, excess heat at moderate temperatures is available, leading to the generation of LP, MP, and HP steam. Further details on heat integration are provided in Section S.4 of the Supplementary Materials.

Economic performance

Fig. 7 summarizes the CAPEX and its breakdown for all scenarios. For the 0 %TS and 20 %TS scenarios, the electrolyser is the primary cost driver, accounting for 48 % and 44 % of the total CAPEX, respectively. As the amount of CO_2 sent for storage increases, the overall CAPEX decreases due to reduced plant productivity and equipment size. However, this reduction is not linear. At 50 %TS, the addition of an ASU to supplement oxygen supply slows down the CAPEX reduction. For scenarios with 40 % or more CO_2 storage, the "RWGS, FT, and upgrading" section becomes the dominant CAPEX contributor. Notably, the CAPEX for CO_2 compression remains relatively low, even for scenarios with significant CO_2 storage. This suggests that adding CCS does not significantly increase the overall cost.

Fig. 8 presents the normalized OPEX per MJ of SAF and its breakdown for all scenarios. The 0 %TS scenario incurs the highest OPEX, while the 100 %TS scenario has the lowest. As more CO_2 is stored, the OPEX decreases due to reduced hydrogen demand. Across all scenarios, wind electricity is the dominant cost driver, contributing between 65 % (0 %TS) and 47 % (100 %TS) of the total OPEX. Forest residue chips are the second-largest cost component, accounting for 11 % and 21 % for the 0 %TS and 100 %TS scenarios, respectively. While the 100 %TS scenario has the highest cost for CO_2 transport and storage, it only accounts for 3 % of the total OPEX. In conclusion, the OPEX of the proposed SAF production scenarios is heavily reliant on electricity costs, and the addition of CCS does not significantly affect operational expenditures. Therefore, substantial OPEX reductions depend on lowering electricity costs.

Despite variations in productivity across scenarios, the MJSP remains relatively consistent, as shown in Fig. 9. The addition of an ASU in certain scenarios significantly affects the CAPEX. However, the MJSP is

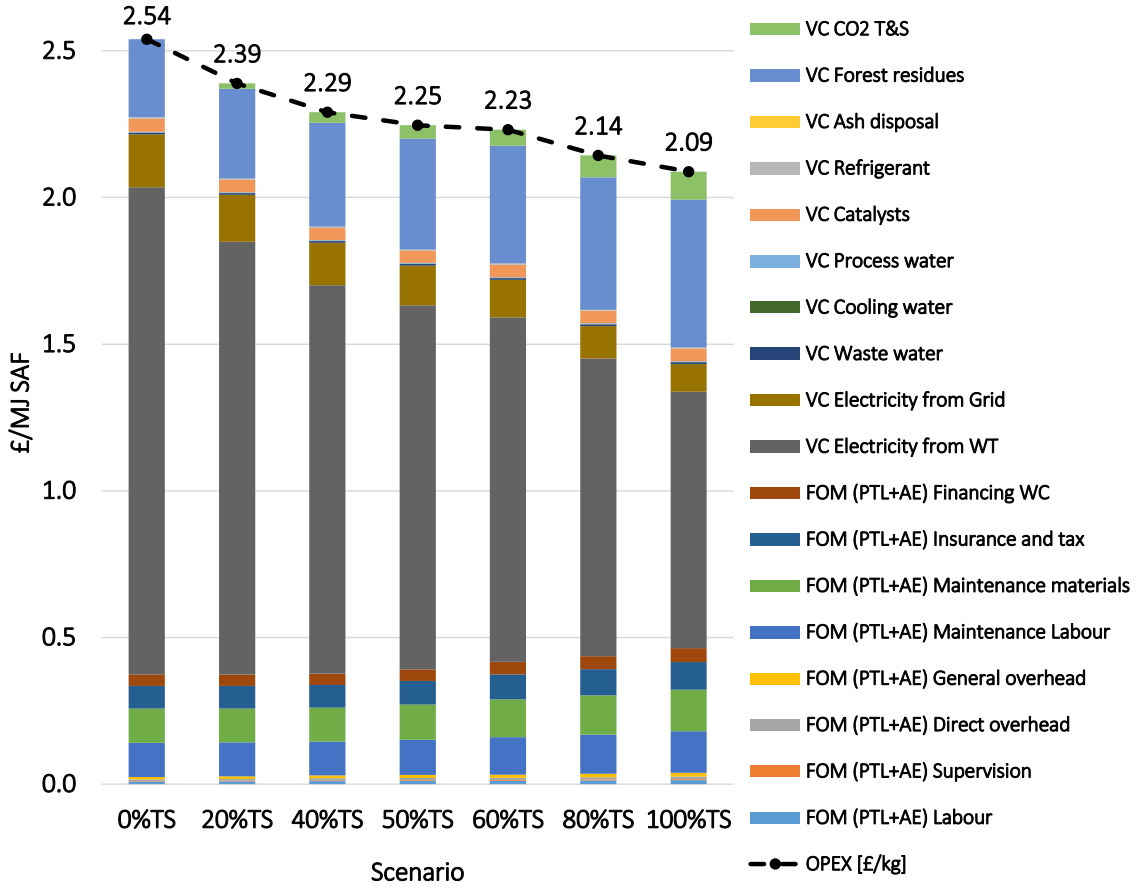

Fig. 8. OPEX breakdown for the different scenarios, in £/MJ of SAF.

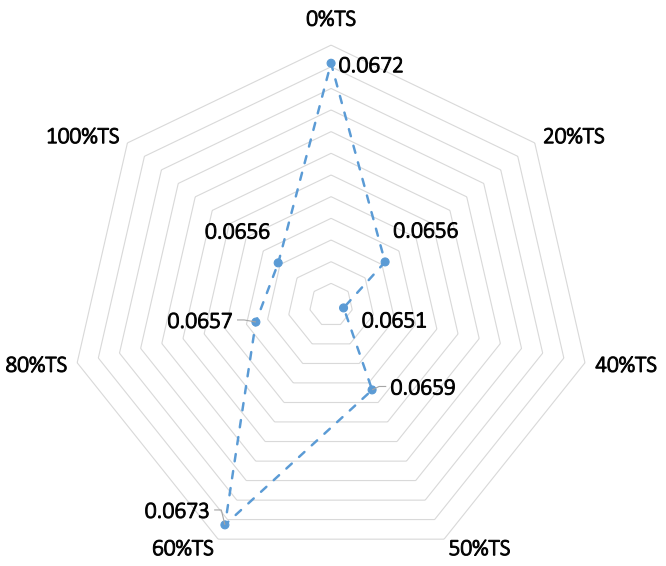

Fig. 9. MJSP for the scenarios in £/MJ of SAF.

primarily driven by OPEX (74 % to 88 %), making it electricity-dependent. While none of the scenarios are cost-competitive with fossil jet fuel (priced at 0.0131 £/MJ [92]), they offer lower MJSPs compared to PtL SAF production [60]. Notably, the addition of CCS has a minimal impact on the final MJSP, highlighting the potential of PBtL-CCS as a negative emissions technology. Previous studies on PBtL configurations report a wide range of economic performance indicators due to varying technology choices, process configurations, and final products. For PBtL-SAF production, the reported selling price ranges from 0.0290 to 0.0636 £/MJ [19,30]. The MJSPs calculated in this study fall within the upper range of these values. These studies also emphasize the significant impact of OPEX, particularly electricity and feedstock costs, on the overall MJSP.

MJSP sensitivity and uncertainty analyses

Fig. 10 presents the results of the sensitivity analysis on the MJSP. The production cost of hydrogen, the electricity cost, and the refinery's CAPEX are the primary drivers of MJSP variation across all scenarios. Given that hydrogen production is the largest electricity consumer, the MJSP is highly sensitive to electricity prices, especially for the 0 %TS scenario with the highest power demand. Additionally, selling naphtha and diesel at the same price as SAF significantly reduces the MJSP. This strategy could encourage the use of renewable naphtha and diesel while lowering SAF production costs. For a more detailed analysis of the sensitivity of the MJSP to hydrogen and forest residue costs, please refer to Section S.7 of the Supplementary Materials.

A probabilistic estimation of the MJSP is presented in Table 8. Due to the wide range assigned to the hydrogen production cost, the standard deviations are relatively high, resulting in a wide range of potential MJSP values. The mean values are higher than those estimated in the deterministic economic assessment, reflecting the impact of hydrogen cost uncertainty. Additionally, the lower range of the confidence intervals indicates that even under optimistic conditions, the PBtL-CCS scenarios may not be economically feasible.

Table 8
Monte Carlo results for the estimation of the MJSP.

Scenario	Mean	Median	Standard Deviation	95 % Confidence Interval	Units
0 %TS	0.087	0.084	0.032	0.025 to 0.149	£/MJ of SAF
20 %TS	0.083	0.080	0.028	0.028 to 0.137	
40 %TS	0.079	0.077	0.024	0.031 to 0.126	
50 %TS	0.078	0.076	0.023	0.034 to 0.122	
60 %TS	0.078	0.077	0.021	0.037 to 0.119	
80 %TS	0.075	0.074	0.018	0.040 to 0.109	
100 %TS	0.072	0.072	0.015	0.044 to 0.101	

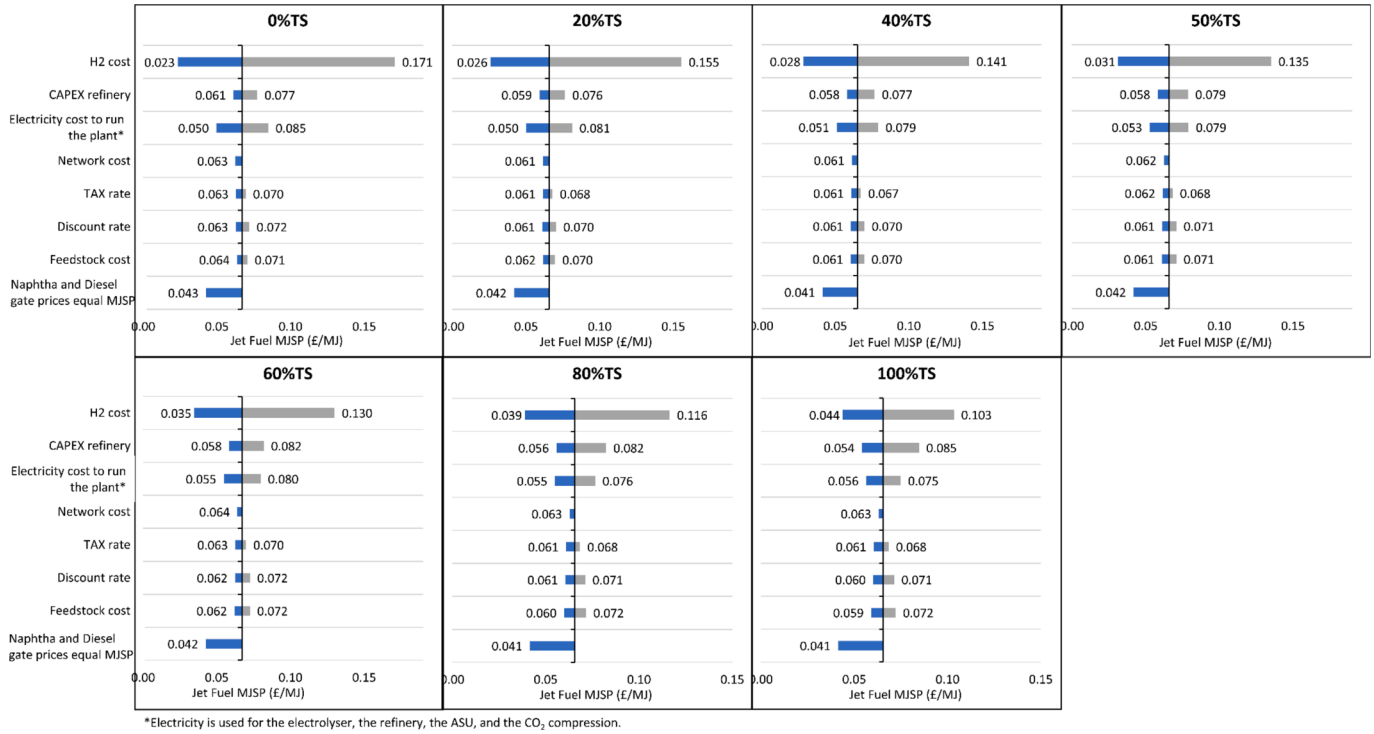

Fig. 10. Sensitivity analysis on the MJSP for the various scenarios.

Environmental performance

The Recipe Midpoint (H) method calculated 18 environmental impacts, from which two are discussed in the main manuscript, while the others are presented in the Supplementary Materials, Section S.8, calculated using the allocation Approach 1 (baseline allocation approach).

Global warming potential (GWP)

Fig. 11 presents the GWP results for different scenarios, calculated using two allocation approaches outlined in Table 4. The baseline allocation approach (Approach 1, orange points) attributes net negative CO_2 emissions solely to SAF, leading to a more negative WtWa GWP for each scenario. In contrast, Approach 1B (blue points) distributes these emissions among SAF, naphtha, and diesel based on their energy content. Given the primary focus on SAF production and the aviation industry's "Net-Zero" target by 2050, the results from Approach 1 are considered the main WtWa GWP values and serve as the basis for sensitivity analyses and subsequent discussions. Regardless of the allocation method, the total amount of net negative CO_2 stored remains constant: 17,464 tCO_2/y for 20 %TS and 126,214 tCO_2/y for 100 %TS.

Fig. 12 breaks down the GWP by LCA stage for each scenario, differentiating between emissions from wind farm electricity and other sources. Excluding CO_2 storage, wood chip production and transport, and wind electricity for AE operation are the primary GWP contributors (orange bars in Fig. 12). Even without CO_2 storage, the 0 %TS scenario achieves a significantly low GWP (13.93 gCO_{2eq}/MJ) compared to PtL SAF [60] and is relatively close to BtL SAF [37]. All scenarios meet emissions reduction thresholds set by RED II [93], the Renewable Fuels Standard (RFS) [94], and the UK SAF mandate [39]. While previous research has addressed GWP estimation for PBtL scenarios, specific LCAs for PBtL-CCS configurations are limited. Habermeyer et al. [20,30] conducted carbon accounting for key WtWa stages, highlighting the significant impact of green electricity on final specific fuel emissions, aligning with the 0 %TS scenario results.

Sensitivity analysis of the GWP

Fig. 13 presents the results of the sensitivity analysis on the GWP. The carbon footprint of wind farm electricity is the primary driver of GWP variation. Additionally, the figure compares GWP results for different allocation approaches (Table 4) and electricity sources. While the choice of allocation method has a minor impact, using grid electricity significantly increases the GWP for all configurations. However, even with grid electricity, scenarios like 50 %TS, 60 %TS, 80 %TS, and 100 %TS still meet the 50 % emissions reduction threshold of the SAF mandate. Furthermore, neglecting upstream emissions of wind electricity, as suggested by the SAF mandate, leads to low GWP values for all scenarios. Given that electricity consumption is the main contributor to GWP, Section S.9 of the Supplementary Materials provides a detailed analysis of the sensitivity of WtWa GWP to different electricity sources and system power requirements for other scenarios.

Furthermore, a probabilistic estimation of the GWP derive in the results of Table 9. Despite the uncertainty of the selected parameters, the estimated mean is similar to the estimated values from the deterministic assessments for all the scenarios. Moreover, the resulting standard deviations lead to the conclusion that in a 95 % confidence interval, the range of estimated GWPs are always negative, except for the 0 %TS, that despite possessing a positive GWP, the resulting probabilistic estimations shows that it will always satisfy even the most severe emissions reduction limits of the proposed SAF mandate.

Water footprint

Fig. 14 depicts the water footprint, differentiating between contributions from wind electricity and other sources for each stage in each scenario. Across all scenarios, the refinery and AE account for over 90 % of total water consumption. For the AE, both electricity consumption

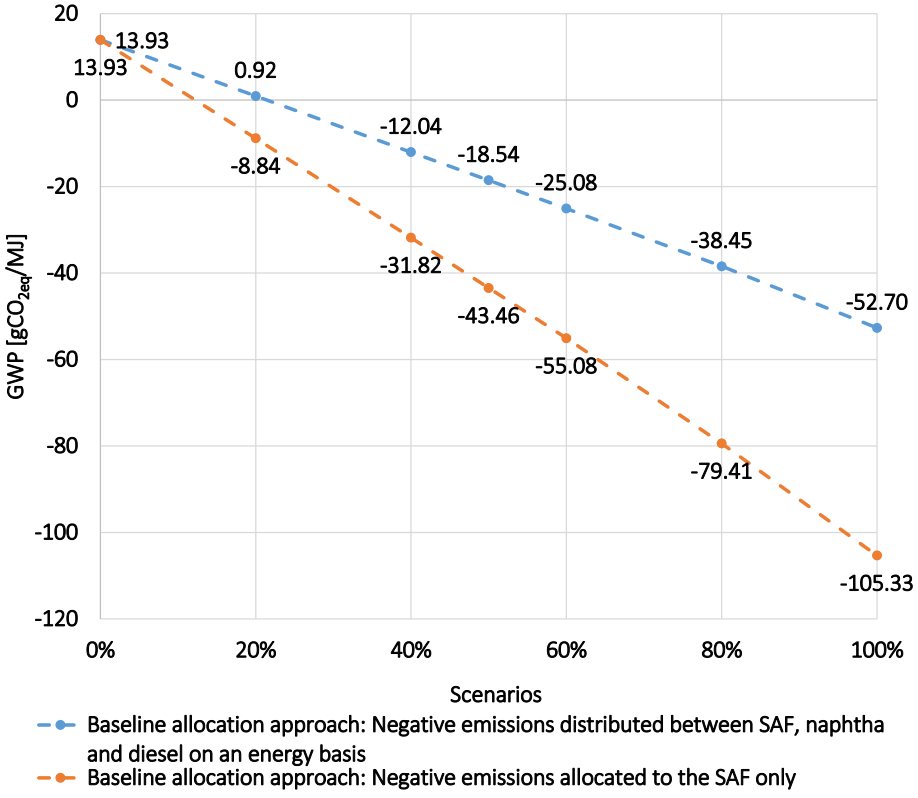

Fig. 11. GWP as a result of the main and second approach for the attribution of negative emissions, upon the "baseline scenario" (as defined in Table 4) allocation method.

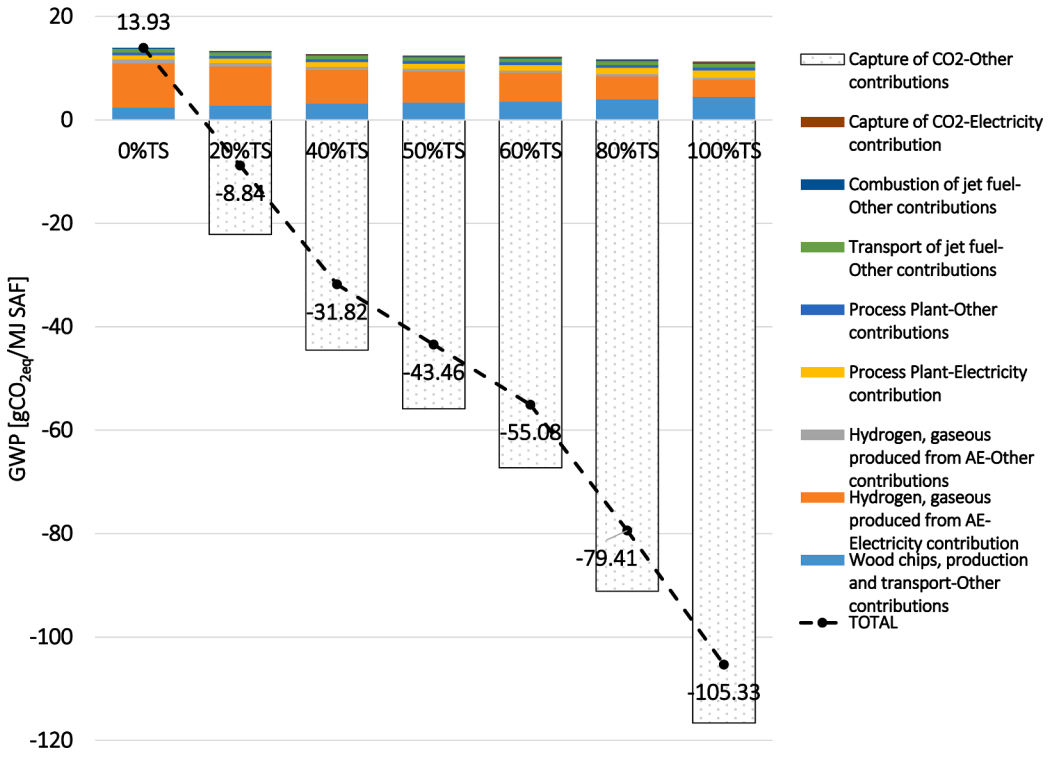

Fig. 12. Breakdown of GWP for the various scenarios.

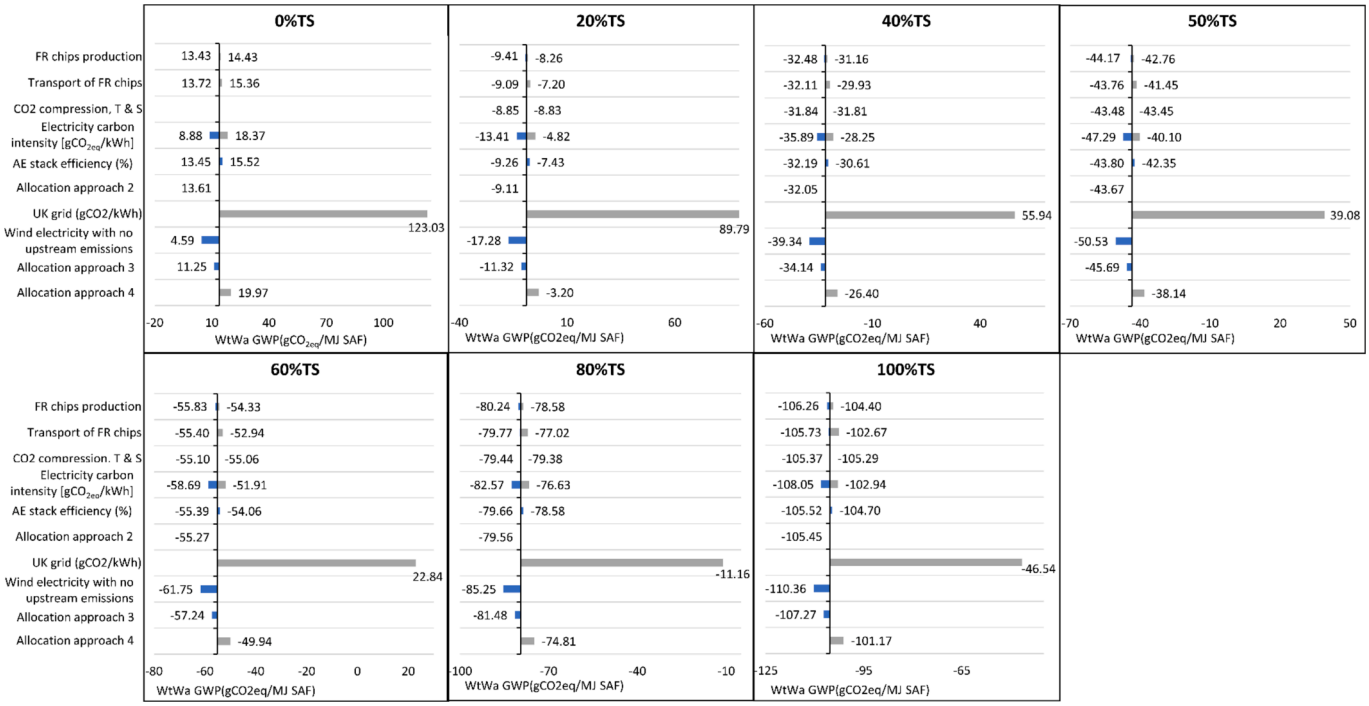

Fig. 13. Sensitivity analysis on the GWP for the proposed scenarios.

and water required for electrolysis contribute equally to the total water footprint. In the refinery plant, the water footprint of electricity consumption is negligible, while makeup water for steam and cooling cycles accounts for 97 % and 94 % in the 0 %TS and 100 %TS scenarios, respectively. While forest residue production and transport have a minimal impact on the final water footprint, other biogenic feedstocks like maize or wheat could significantly increase water consumption [95]. The 100 %TS scenario, with its lower hydrogen requirement and reduced electricity consumption, has the lowest water footprint among all the configurations.

The refinery plant is the primary contributor to the water footprint. Strategies like air-cooling could reduce this, but their performance is sensitive to humidity and temperature [96]. Alternatively, water synthesised and recovered from the process could supply the electrolyser,

Table 9
Monte Carlo results for the estimation of the GWP.

Scenario	Mean	Median	Standard Deviation	95 % Confidence Interval	Units
0 %TS	14.43	14.47	2.02	10.47 to 18.40	gCO_{2eq}/ MJ
20 %TS	−8.24	−8.22	1.85	−11.86 to −4.62	
40 %TS	−31.17	−31.15	1.68	−34.47 to −27.88	
50 %TS	−42.79	−42.78	1.60	−45.93 to −39.65	
60 %TS	−54.39	−54.38	1.54	−57.40 to −51.37	
80 %TS	−78.67	−78.68	1.41	−81.44 to −75.90	
100 %TS	−104.54	−104.55	1.31	−107.11 to −101.97	

Note: Equation 7,8,9 change to Equation (4),5,6 kindly check.

reducing freshwater inputs. However, wastewater would require treatment to reduce hydrocarbon content. Fig. 15 shows that wind electricity minimizes the water footprint compared to solar, nuclear, or hydropower. Nonetheless, all scenarios have higher water footprints than fossil jet fuel (0.0632 l/MJ).

Policy analysis: SAF mandate and negative emissions trading system

This section assesses the impact of the UK SAF mandate on the economic performance of the SAF production scenarios. While the final mandate is expected to be put on place in 2025, the response of the government to the second consultation [34,97] is applied here. The SAF mandate aims to support the UK's Net-Zero Strategy by achieving net-zero aviation emissions by 2050 [98]. The Jet Zero Strategy proposes replacing 10 % of conventional jet fuel with SAF by 2030 and reaching a 50 % SAF uptake by 2050 [97]. SAF must be a drop-in fuel with a 70 % emissions reduction compared to conventional jet fuel, derived from sustainable, non-food feedstocks that avoid deforestation [39,99,100]. This aligns with the use of forest residues in the analysed scenarios, making them eligible for SAF mandate incentives.

The SAF mandate offers economic support through tradable certificates with a market-determined value to bridge the gap between SAF and jet fuel prices [39]. Equation (4) [39] describes the methodology for the calculation of the amount of certificates; this is proportional to the energy content of the SAF, represented by the term $m_{SAF} \times LHV_{SAF}$ (where m_{SAF} is the mass of the SAF produced and LHV_{SAF} the SAF low heating value, which is fixed at 42.8 MJ/kg [62]). The number of certificates awarded is proportional to a carbon intensity factor,(CI_{factor}), which is itself a function of the carbon intensity of the fuel (CI_{SAF}), as depicted in Equation (5). The CI_b is the carbon intensity of a benchmark SAF that achieves 70 % emission reduction, i.e. 26.7 gCO_{2eq}/MJ, and the CI_F is the carbon intensity of the fossil jet fuel, i.e. 89 gCO_{2eq}/MJ [39].

$$\text{Number of certificates} = m_{SAF} \times LHV_{SAF} \times CI_{factor} \quad (4)$$

$$CI_{factor} = \frac{CI_F - CI_{SAF}}{CI_F - CI_b} \quad (5)$$

$$CI_{factor} = \frac{CI_F - \text{If}\,(CI_{SAF} \geq 0,\ CI_{SAF},\ 0)}{CI_F - CI_b} \quad (6)$$

Under the current stage of the SAF mandate, there is not yet any provision to account for net negative emissions. It is still under discussion whether these negative emissions should be recognized and awarded under the same SAF mandate or another additional policy should reward these BECCS-SAF scenarios [39]. Therefore, to align with this statement, for the six investigated scenarios with negative emissions, the CI_{factor} could be also calculated by assuming that the GWP is zero, as shown in Equation (6). In this sense, two sets of results are presented: 1) Recognising the negative emissions of the scenarios and using Equation (5), 2) Disregarding the negative emissions and using Equation (6) instead.

Fig. 16 presents the results for the 0 %TS scenario, illustrating the variability of certificate prices under different electricity costs and carbon footprints. The figure highlights that higher electricity costs and carbon footprints lead to higher certificate prices, emphasizing the

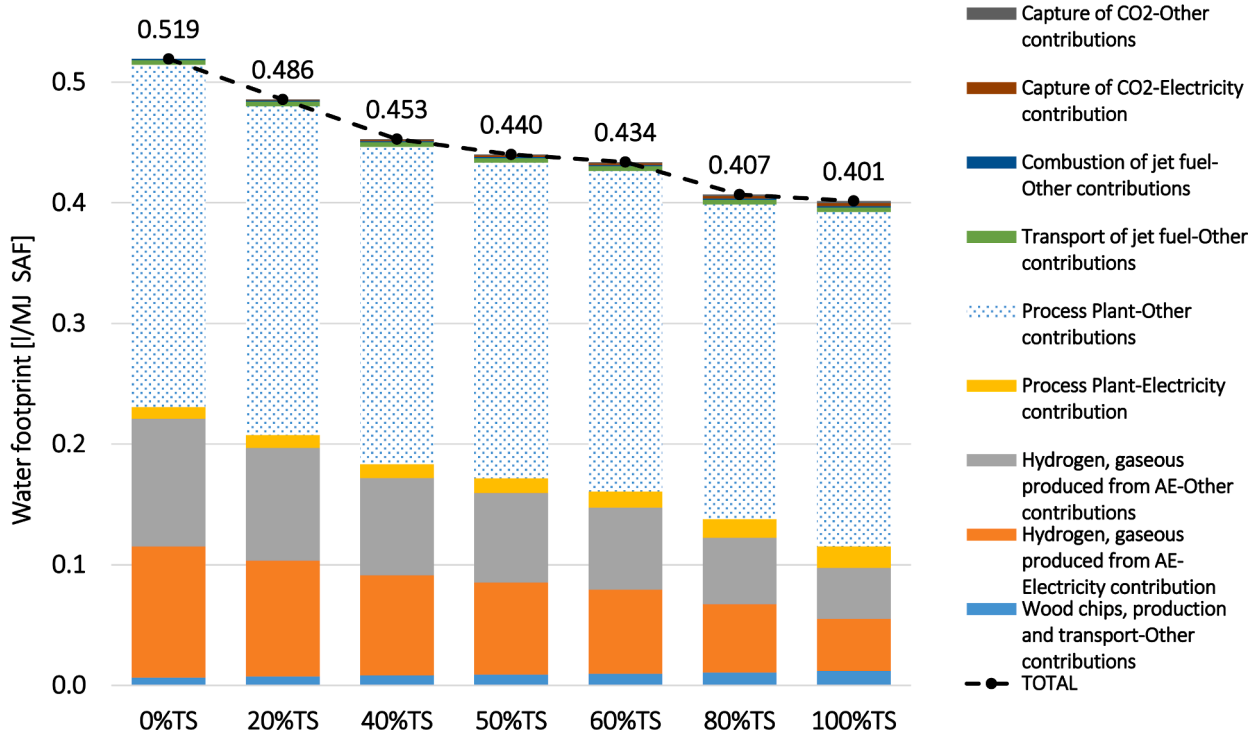

Fig. 14. Water footprint breakdown for the different scenarios.

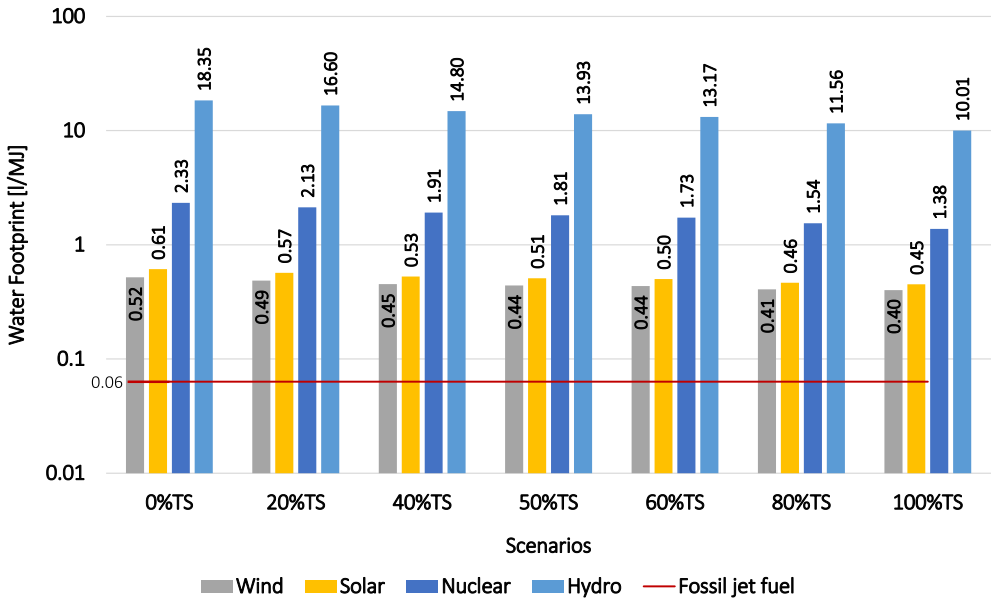

Fig. 15. Water footprint of the PBtL-CCS scenarios when connected to different electricity sources.

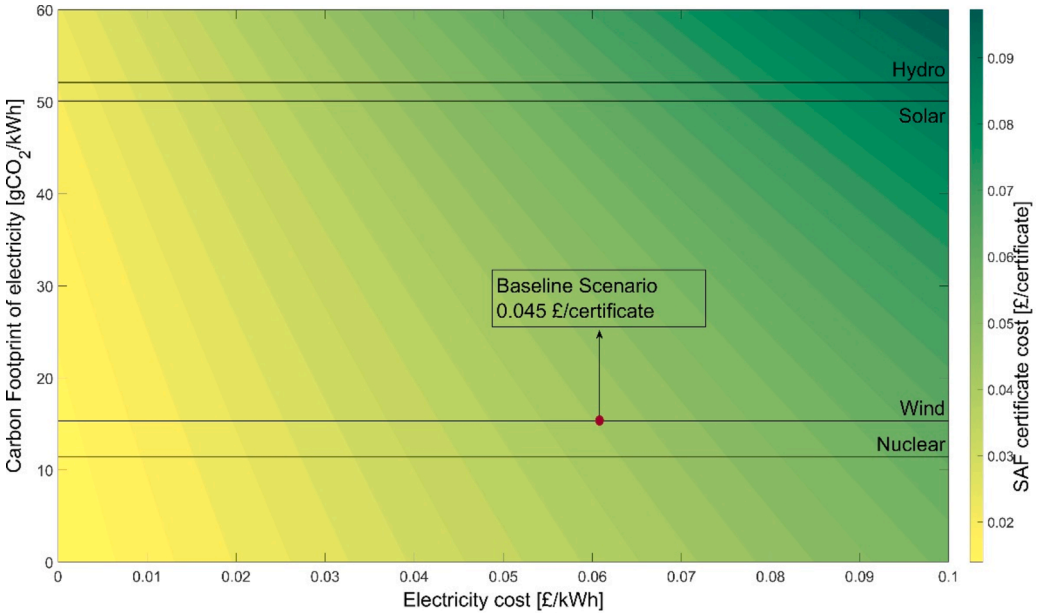

Fig. 16. The price of SAF certificates that would need to be set in order for the MJSP to be profitable at the current gate price of fossil jet fuel (0.56£/kg), for different electricity costs and electricity carbon footprint, under the 0 %TS scenario.

importance of affordable and low-GHG electricity.

Fig. 17 illustrates the certificate costs for the 50 %TS and 100 %TS scenarios, which, due to their negative GWP, have significantly lower costs. In Fig. 17B and 19D, the certificate cost remains constant for each electricity cost, regardless of its GWP, as Equation (6) assigns a value of 0. Recognizing negative emissions from BECCS configurations can enhance the economic viability of these processes by enabling them to break even with fossil jet fuel at lower certificate prices. The second consultation of the SAF mandate considered whether to include upstream emissions of electricity sources in SAF carbon accounting. This could potentially equate renewable energy emissions at the point of delivery to zero. However, this consideration is primarily limited to nuclear energy [39]. If implemented, this could lead to a higher number of certificates awarded for each scenario, resulting in lower certificate prices.

Conclusions

As biomass availability may limit SAF production capacity, hybridising biomass to liquid (BtL) with power to liquid (PtL) can increase fuel yields and dampen production costs. While previous research indicates that SAF production pathways can reduce emissions, this is not enough for the aviation industry to achieve net-zero targets and hence carbon dioxide removal (CDR) technologies need to be deployed. To this direction, the proposed power and biomass to liquids coupled with carbon capture and storage (PBtL-CCS) route is a novel process configuration that can both produce SAF and also achieve negative emissions. We have developed a new design for SAF production that can exploit the advantages of the PBtL and at the same time to sequestrate biogenic CO_2.

Several configurations have been assessed and it was found that even for the cases that the design assumes relatively lower CO_2 storage flows,

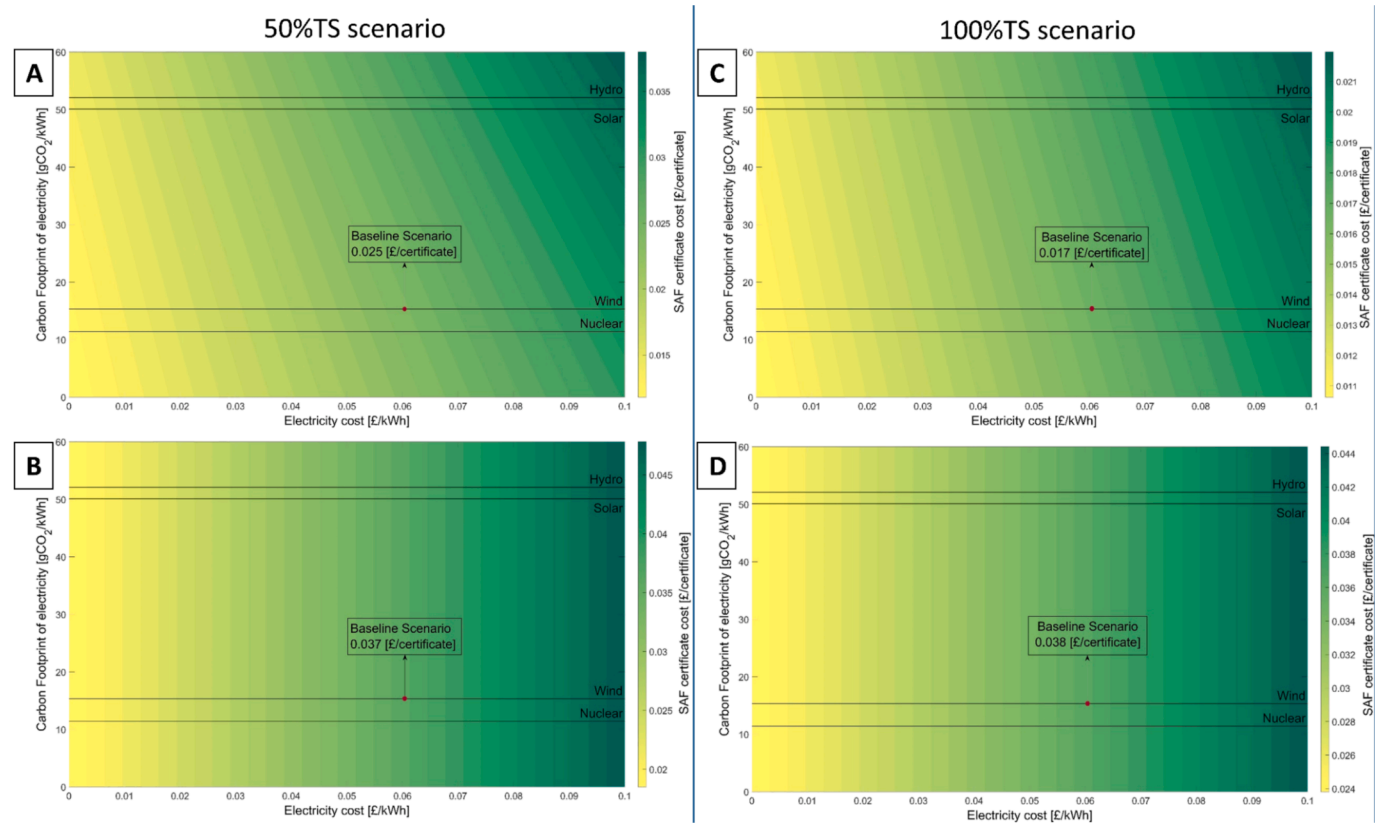

Fig. 17. The price of SAF certificates that would need to be set in order for the MJSP to be profitable at the current gate price of fossil jet fuel (0.56£/kg), for different electricity costs and electricity carbon footprint, for the: A) 50 %TS scenario, acknowledging the negative GWP; B) 50 %TS scenario, without acknowledging the negative GWP; C) 100 %TS scenario, acknowledging the negative GWP; and D) 100 %TS scenario, without acknowledging the negative GWP.

negative global warming potential (GWP) values can be attained based on a comprehensive well-to-wake LCA. Key findings of this research include:

1. The PBtL-CCS process achieved high carbon conversion efficiencies (55–99 %), exceeding BtL and comparable to PtL. However, as expected CCS negatively impacts the carbon efficiency due to reduced SAF production. Hydrogen conversion efficiency is in the range of 21.5 to 22.6 % due to water formation in reactions.
2. PBtL and PBtL-CCS configurations are energy-intensive, particularly the 0 %TS scenario. Increased CO_2 storage improves energy efficiency, especially in the 100 %TS scenario. This is because more H_2 is needed for the reverse water gas shift (RWGS) reaction for the cases that they store less CO_2. It should be noted that CO_2 compression requires relatively lower electricity, making hydrogen production the primary energy consumer.
3. The MJSP ranges from 0.0651 to 0.0673 £/MJ and is primarily driven by OPEX, particularly electricity costs. Sensitivity analysis indicates that reducing electricity costs significantly lowers the MJSP. Monte Carlo analysis reveals high uncertainty in the MJSP, with wide 95 % confidence intervals.
4. The 0 %TS scenario has a GWP of 13.93 gCO_{2eq}/MJ, which is significantly lower than fossil jet fuel and meets stringent emission reduction thresholds. However, to achieve net-zero emissions, CCS scenarios are more suitable. These scenarios have GWPs ranging from −8.84 to −105.33 gCO_{2eq}/MJ of SAF. Monte Carlo simulations confirm the robustness of these results.
5. The water footprint is primarily influenced by electricity source, electrolysis water requirements, and refinery processes. CO_2 storage has minimal impact. The 100 %TS scenario has the lowest water footprint (0.40 l/MJ), while the 0 %TS scenario has the highest (0.52 l/MJ). Wind energy is the most water-efficient renewable electricity source, but still all scenarios have significantly higher water footprints than fossil jet fuel (0.0632 l/MJ).
6. The use of policies such as the SAF mandate certificate trading scheme could help on achieving more affordable SAF, especially when the negative emissions are also rewarded, demonstrating the advantage of the CCS scenarios over the normal PBtL configuration.

The study provides a holistic assessment that includes technical modelling, techno economic and LCA assessment as well as consideration of policy schemes of a novel SAF route and can provide valuable insights to pilot testing, scale-up, and policy making. Adding a CCS supply chain minimally affects economics but positively affects the environmental footprint by a great deal. The proposed PBtL-CCS system provides a new pathway to achieve negative emissions, contributing to the aviation sector's net-zero goals. Future research should focus on pilot testing, considering evolving energy markets, and assessing the impact of climate change and land use policies on biomass availability. Additionally, as proposed herein business models that incentivise carbon-negative processes can enhance the economic viability of PBtL-CCS.

CRediT authorship contribution statement

Maria Fernanda Rojas-Michaga: Writing – original draft, Validation, Resources, Methodology, Formal analysis, Conceptualization. **Stavros Michailos:** Conceptualization, Methodology, Software, Investigation, Validation, Writing – review & editing. **Evelyn Cardozo:** Methodology, Software, Writing – review & editing. **Kevin J. Hughes:** Writing – review & editing, Supervision, Resources. **Derek Ingham:** Project administration, Resources, Supervision, Writing – review &

editing. **Mohamed Pourkashanian:** Resources, Supervision, Writing – review & editing.

Declaration of competing interest

The authors declare that they have no known competing financial interests or personal relationships that could have appeared to influence the work reported in this paper.

Acknowledgements

The second author is grateful to the R and I Support Fund provided by University of Hull United Kingdom and the UKCCSRC Flexible Funding 2020. In addition, the contribution of the UK Industrial Decarbonisation Research and Innovation Centre (IDRIC) is much acknowledged and appreciated.

Appendix A. Supplementary data

Supplementary data to this article can be found online at https://doi.org/10.1016/j.ecmx.2024.100841.

Data availability

Data will be made available on request.

References

[1] Mission Possible, "Making Net-Zero Aviation Possible," 2022. Accessed: May 19, 2023. [Online]. Available: https://missionpossiblepartnership.org/wp-content/uploads/2023/01/Making-Net-Zero-Aviation-possible.pdf.
[2] The Royal Society, "Net zero aviation fuels: Resource requirements and environmental impacts," 2023. Accessed: Apr. 24, 2023. [Online]. Available: https://royalsociety.org/-/media/policy/projects/net-zero-aviation/net-zero-aviation-fuels-policy-briefing.pdf.
[3] IATA, "Our Commitment to Fly Net Zero by 2050," Jul. 19, 2023. https://www.iata.org/en/programs/environment/flynetzero/ (accessed Jul. 19, 2023).
[4] Aviation Environment Federation, "IATA announces net zero emissions by 2050 target for global air transport industry," Jul. 19, 2023.
[5] Carbon Direct, "Sustainable Aviation Fuels Primer: Promising production pathways and opportunities to scale," 2023. Accessed: Aug. 22, 2023. [Online]. Available: https://www.carbon-direct.com/insights/a-primer-on-the-future-of-sustainable-aviation-fuel.
[6] De Jong S, Antonissen K, Hoefnagels R, Lonza L, Wang M, Faaij A, et al. Life-cycle analysis of greenhouse gas emissions from renewable jet fuel production. *Biotechnol Biofuels* 2017;10(1):1–18. https://doi.org/10.1186/s13068-017-0739-7.
[7] Rojas-Michaga MF, Michailos S, Hughes KJ, Ingham D, Pourkashanian M. Techno-economic and life cycle assessment review of sustainable aviation fuel produced via biomass gasification. *Sustainable Biofuels* 2021. https://doi.org/10.1016/b978-0-12-820297-5.00012-8.
[8] Neuling U, Kaltschmitt M. Techno-economic and environmental analysis of aviation biofuels. *Fuel Process Technol* 2018;171(September 2017):54–69. https://doi.org/10.1016/j.fuproc.2017.09.022.
[9] Ahire JP, Bergman R, Runge T, Mousavi-Avval SH, Bhattacharyya D, Brown T, et al. Techno-economic and environmental impacts assessments of sustainable aviation fuel production from forest residues. *Sustain Energy Fuels* 2024;8(19):4602–16. https://doi.org/10.1039/D4SE00749B.
[10] Tijmensen MJA, Faaij APC, Hamelinck CN, Van Hardeveld MRM. Exploration of the possibilities for production of Fischer Tropsch liquids and power via biomass gasification. *Biomass Bioenergy* 2002;23(2):129–52. https://doi.org/10.1016/S0961-9534(02)00037-5.
[11] Anex RP, Aden A, Kazi FK, Fortman J, Swanson RM, Wright MM, et al. Techno-economic comparison of biomass-to-transportation fuels via pyrolysis, gasification, and biochemical pathways. *Fuel* 2010;89(1):S29–35. https://doi.org/10.1016/j.fuel.2010.07.015.
[12] Diederichs GW, Ali Mandegari M, Farzad S, Görgens JF. Techno-economic comparison of biojet fuel production from lignocellulose, vegetable oil and sugar cane juice. *Bioresour Technol* 2016;216:331–9. https://doi.org/10.1016/j.biortech.2016.05.090.
[13] Micheli M, Moore D, Bach V, Finkbeiner M. Life-Cycle Assessment of Power-to-Liquid Kerosene Produced from Renewable Electricity and CO2 from Direct Air Capture in Germany. *Sustainability (switzerland)* 2022;14(17). https://doi.org/10.3390/su141710658.
[14] M. F. Rojas-Michaga, S. E. Michailos, E. Cardozo, M. Akram, K. J. Kevin Hughes, D. B. Ingham, *et al.*, "Sustainable aviation fuel (SAF) production through power-to-liquid (PtL): A combined techno-economic and life cycle assessment," *Energy Convers Manag*, vol. 292, 2023, doi: 10.1016/j.enconman.2023.117427.
[15] V. Batteiger, K. Ebner, A. Habersetzer, L. Moser, P. Schmidt, W. Weindorf, *et al.*, "Power-to-Liquids – A scalable and sustainable fuel supply perspective for aviation," 2022. [Online]. Available: https://www.umweltbundesamt.de/en/publications.
[16] P. R. Schmidt, W. Zittel, W. Weindorf, and T. Raksha, "Empowering a sustainable mobility future with zero emission fuels from renewable electricity," p. 203, 2016.
[17] M. Fasihi and O. A. Solomon, "E-Kerosene for Commercial Aviation From Green Hydrogen and CO 2 from Direct Air Capture – Volumes , Cost ," no. September, 2022.
[18] Eyberg V, Dieterich V, Bastek S, Dossow M, Spliethoff H, Fendt S. Techno-economic assessment and comparison of Fischer–Tropsch and Methanol-to-Jet processes to produce sustainable aviation fuel via Power-to-Liquid. *Energy Convers Manag* 2024;315:118728. https://doi.org/10.1016/j.enconman.2024.118728.
[19] Dietrich RU, Albrecht FG, Maier S, König DH, Estelmann S, Adelung S, et al. Cost calculations for three different approaches of biofuel production using biomass, electricity and CO2. *Biomass Bioenergy* 2018;111:165–73. https://doi.org/10.1016/j.biombioe.2017.07.006.
[20] Habermeyer F, Papantoni V, Brand-Daniels U, Dietrich RU. Sustainable aviation fuel from forestry residue and hydrogen - a techno-economic and environmental analysis for an immediate deployment of the PBtL process in Europe. *Sustain Energy Fuels* 2023;7(17):4229–46. https://doi.org/10.1039/d3se00358b.
[21] M. Hillestad, M. Ostadi, G. D. Alamo Serrano, E. Rytter, B. Austbø, J. G. Pharoah, *et al.*, "Improving carbon efficiency and profitability of the biomass to liquid process with hydrogen from renewable power," *Fuel*, vol. 234, pp. 1431–1451, Dec. 2018, doi: 10.1016/j.fuel.2018.08.004.
[22] Mesfun S, Engvall K, Toffolo A. Electrolysis Assisted Biomass Gasification for Liquid Fuels Production. *Front Energy Res* 2022;10. https://doi.org/10.3389/fenrg.2022.799553.
[23] Schulzke T. Synergies from direct coupling of biomass-to-liquid and power-to-liquid plants. *Chem Eng Technol* 2017;40(2):254–9. https://doi.org/10.1002/ceat.201600179.
[24] Ostadi M, Austbø B, Hillestad M. Parametric Optimization of a Power and Biomass to Liquid Process. Computer Aided Chemical Engineering Elsevier bv 2019:287–92. https://doi.org/10.1016/B978-0-12-818597-1.50045-X.
[25] Ostadi M, Rytter E, Hillestad M. Boosting carbon efficiency of the biomass to liquid process with hydrogen from power: The effect of H2/CO ratio to the Fischer-Tropsch reactors on the production and power consumption. *Biomass Bioenergy* Aug. 2019;127. https://doi.org/10.1016/j.biombioe.2019.105282.
[26] Ostadi M, Austbø B, Hillestad M. Exergy analysis of a process converting power and biomass to a liquid fuel. *Chem Eng Trans* 2019;76:205–10. https://doi.org/10.3303/CET1976035.
[27] Nielsen AS, Ostadi M, Austbø B, Hillestad M, del Alamo G, Burheim O. Enhancing the efficiency of power- and biomass-to-liquid fuel processes using fuel-assisted solid oxide electrolysis cells. *Fuel* 2022;321. https://doi.org/10.1016/j.fuel.2022.123987.
[28] Ostadi M, Paso KG, Rodriguez-Fabia S, Øi LE, Manenti F, Hillestad M. Process integration of green hydrogen: Decarbonization of chemical industries. *Energies (basel)* 2020;13(18). https://doi.org/10.3390/en13184859.
[29] Weyand J, Habermeyer F, Dietrich RU. Process design analysis of a hybrid power-and-biomass-to-liquid process – An approach combining life cycle and techno-economic assessment. *Fuel* 2023;342. https://doi.org/10.1016/j.fuel.2023.127763.
[30] Habermeyer F, Weyand J, Maier S, Kurkela E, Dietrich RU. Power Biomass to Liquid — an option for Europe's sustainable and independent aviation fuel production. *Biomass Convers Biorefin* 2023. https://doi.org/10.1007/s13399-022-03671-y.
[31] Dossow M, Dieterich V, Hanel A, Spliethoff H, Fendt S. Improving carbon efficiency for an advanced Biomass-to-Liquid process using hydrogen and oxygen from electrolysis. *Renew Sustain Energy Rev* 2021;152. https://doi.org/10.1016/j.rser.2021.111670.
[32] Staples MD, Isaacs SA, Allroggen F, Mallapragada DS, Falter CP, Barrett SRH. Environmental and economic performance of hybrid power-to- liquid and biomass-to-liquid fuel production in the united states. *Environ Sci Technol* 2021;55(12):8247–57. https://doi.org/10.1021/acs.est.0c07674.
[33] Shahrivar M, Saeed MN, Surywanshi GD, Mattisson T, Soleimanisalim AH. Improving bio aviation fuel yield from biogenic carbon sources through electrolysis assisted chemical looping gasification. *Fuel* 2023;348:128525. https://doi.org/10.1016/j.fuel.2023.128525.
[34] Ishaq M, Dincer I. A novel integrated gas-cooled fast nuclear reactor and vanadium chloride thermochemical cycle for sustainable fuel production. *J Clean Prod* 2024;468:142853. https://doi.org/10.1016/j.jclepro.2024.142853.
[35] Voß S, Bube S, Kaltschmitt M. Hybrid Biomass- and Electricity-Based Kerosene Production—A Techno-Economic Analysis. *Energy Fuel* 2024;38(6):5263–78. https://doi.org/10.1021/acs.energyfuels.3c04876.
[36] IPCC, "Global warming of 1.5°C: An IPCC Special Report on the impacts of global warming of 1.5°C above pre-industrial levels and related global greenhouse gas emission pathways, in the context of strengthening the global response to the threat of climate change," 2018. doi: 10.1002/9780470996621.ch50.
[37] Rojas Michaga MF, Michailos S, Akram M, Cardozo E, Hughes KJ, Ingham D, et al. Bioenergy with carbon capture and storage (BECCS) potential in jet fuel production from forestry residues: A combined Techno-Economic and Life Cycle Assessment approach. *Energy Convers Manag* 2022;255(November 2021):115346. https://doi.org/10.1016/j.enconman.2022.115346.

[38] Almena A, Siu R, Chong K, Thornley P, Röder M. Reducing the environmental impact of international aviation through sustainable aviation fuel with integrated carbon capture and storage. *Energy Convers Manag* 2024;303:118186. https://doi.org/10.1016/j.enconman.2024.118186.

[39] Department for Transport, "Pathway to net zero aviation: Developing the UK sustainable aviation fuel mandate A second consultation on reducing the greenhouse gas emissions of aviation fuel in the UK," 2023. [Online]. Available: www.nationalarchives.gov.uk/doc/opengovernment-licence/version/3/.

[40] E4tech, "Advanced drop-in biofuels: UK production capacity outlook to 2030," no. February, p. 83, 2017.

[41] R. Dahl, "Evaluation of the new Power & Biomass to Liquid (PBtL) concept for production of biofuels from woody biomass," 2020.

[42] The Crown Estate's Offshore Wind Evidence and Change Programme, "Future Offshore Wind Future offshore wind scenarios: an assessment of deployment drivers," 2022. Accessed: Aug. 03, 2023. [Online]. Available: https://www.marinedataexchange.co.uk/details/3558/summary.

[43] Scottish Carbon Capture & Storage, "Global CCS Map." https://www.sccs.org.uk/resources/global-ccs-map (accessed Aug. 03, 2023).

[44] The CCUS Hub, "East Coast Cluster," Jul. 28, 2023. https://ccushub.ogci.com/focus_hubs/east-coast-cluster/ (accessed Jul. 28, 2023).

[45] Scott JA, Adams TA. Biomass-gas-and-nuclear-to-liquids (BGNTL) Processes Part I: Model Development and Simulation. *Can J Chem Eng* 2018;96(9):1853–71. https://doi.org/10.1002/cjce.23231.

[46] Michailos S, Walker M, Moody A, Poggio D, Pourkashanian M. Biomethane production using an integrated anaerobic digestion, gasification and CO2 biomethanation process in a real waste water treatment plant: A techno-economic assessment. *Energy Convers Manag* 2020;209(no. March):112663. https://doi.org/10.1016/j.enconman.2020.112663.

[47] Adelung S, Maier S, Dietrich RU. Impact of the reverse water-gas shift operating conditions on the Power-to-Liquid process efficiency. *Sustainable Energy Technol Assess* 2021;43(November 2020):100897. https://doi.org/10.1016/j.seta.2020.100897.

[48] M. Holst, S. Aschbrenner, T. Smolinka, C. Voglstätter, and G. Grimm, "Cost Forecast for Low Temperature Electrolysis - Technology Driven Bottom-up Prognosis for PEM and Alkaline Water Electrolysis Systems," p. 79, 2021.

[49] Young AF, Villardi HGD, Araujo LS, Raptopoulos LSC, Dutra MS. Detailed design and economic evaluation of a cryogenic air separation unit with recent literature solutions. *Ind Eng Chem Res* 2021;60(41):14830–44. https://doi.org/10.1021/acs.iecr.1c02818.

[50] Aspen Technology Inc. and Aspen Plus V 8.4, "Aspen Physical Property System: Physical Property Methods," *Methods*, pp. 1–234, 2013, [Online]. Available: http://profsite.um.ac.ir/~fanaei/_private/Property Methods 8_4.pdf.

[51] Xie J, Zhong W, Jin B, Shao Y, Liu H. Simulation on gasification of forestry residues in fluidized beds by Eulerian-Lagrangian approach. *Bioresour Technol* 2012;121:36–46. https://doi.org/10.1016/j.biortech.2012.06.080.

[52] "MERRA-2." https://gmao.gsfc.nasa.gov/reanalysis/MERRA-2/ (accessed Aug. 29, 2022).

[53] Freeman J, Jorgenson J, Gilman P, Ferguson T. Reference Manual for the System Advisor Model's Wind Power Performance Model. [Online]. Available: www.nrel.gov/publications; 2014.

[54] Pacific Green, "Green hydrogen: why batteries are a key part of the picture." https://www.pacificgreen-energystorage.com/articles/green-hydrogen-why-batteries-are-key-part-picture (accessed Jun. 09, 2022).

[55] Tebibel H. Methodology for multi-objective optimization of wind turbine/battery/electrolyzer system for decentralized clean hydrogen production using an adapted power management strategy for low wind speed conditions. *Energy Convers Manag* 2021;238:114125. https://doi.org/10.1016/j.enconman.2021.114125.

[56] García Clúa JG, Mantz RJ, De Battista H. Optimal sizing of a grid-assisted wind-hydrogen system. *Energy Convers Manag* 2018;166:402–8. https://doi.org/10.1016/j.enconman.2018.04.047.

[57] Olateju B, Kumar A, Secanell M. A techno-economic assessment of large scale wind-hydrogen production with energy storage in Western Canada. *Int J Hydrogen Energy* 2016;41(21):8755–76. https://doi.org/10.1016/j.ijhydene.2016.03.177.

[58] Gökçek M, Kale C. Optimal design of a Hydrogen Refuelling Station (HRFS) powered by Hybrid Power System. *Energy Convers Manag* 2018;161(February):215–24. https://doi.org/10.1016/j.enconman.2018.02.007.

[59] Ursúa A, Barrios EL, Pascual J, San Martín I, Sanchis P. Integration of commercial alkaline water electrolysers with renewable energies: Limitations and improvements. *Int J Hydrogen Energy* 2016;41(30):12852–61. https://doi.org/10.1016/j.ijhydene.2016.06.071.

[60] Rojas-Michaga MF, Michailos S, Cardozo E, Akram M, Hughes KJ, Ingham D, et al. Sustainable aviation fuel (SAF) production through power-to-liquid (PtL): A combined techno-economic and life cycle assessment. *Energy Convers Manag* 2023;292:117427. https://doi.org/10.1016/j.enconman.2023.117427.

[61] Engineering Toolbox, "Fuels - Higher and Lower Calorific Values," 2023. https://www.engineeringtoolbox.com/fuels-higher-calorific-values-d_169.html (accessed Aug. 07, 2023).

[62] ASTM, "Standard Specification for Aviation Turbine Fuel Containing Synthesized Hydrocarbons (ASTM D7566-21)," *Annual Book of ASTM Standards*, pp. 1–38, 2021, doi: 10.1520/D7566-21.operated.

[63] S. Heyne and S. Harvey, "Impact of choice of CO 2 separation technology on thermo-economic performance of Bio-SNG production processes," no. April 2013, pp. 299–318, 2014, doi: 10.1002/er.

[64] Swanson RM, Platon A, Satrio JA, Brown RC. Techno-economic analysis of biomass-to-liquids production based on gasification. *Fuel* 2010;89(SUPPL. 1):S11–9. https://doi.org/10.1016/j.fuel.2010.07.027.

[65] Michailos S, Emenike O, Ingham D, Hughes KJ, Pourkashanian M. Methane production via syngas fermentation within the bio-CCS concept: A techno-economic assessment. *Biochem Eng J* 2019;150(no. May):107290. https://doi.org/10.1016/j.bej.2019.107290.

[66] Baumann H, Tillman A-M. *The Hitch Hiker's Guide to LCA* 2004.

[67] Heijungs R, Allacker K, Benetto E, Brandão M, Guinée J, Schaubroeck S, et al. System Expansion and Substitution in LCA: A Lost Opportunity of ISO 14044 Amendment 2. *Front Sustainability* 2021;2(June):1–3. https://doi.org/10.3389/frsus.2021.692055.

[68] Ecoinvent, "System Models," Jul. 26, 2023. https://ecoinvent.org/the-ecoinvent-database/system-models/ (accessed Jul. 26, 2023).

[69] International Organization for Standardization, "Environmental Management - Life Cycle Assessment - Principles and Framework (ISO 14040:2006)," 2006 doi: 10.1016/j.ecolind.2011.01.007.

[70] Royal Academy of Engineering, "Sustainability of liquid biofuels," 2017.

[71] United Nations Framework Convention on Climate Change, "Methodological tool Apportioning emissions from production processes between main product and co- and by-product," 2015.

[72] Liu CM, Sandhu NK, McCoy ST, Bergerson JA. A life cycle assessment of greenhouse gas emissions from direct air capture and Fischer-Tropsch fuel production. *Sustain Energy Fuels* 2020;4(6):3129–42. https://doi.org/10.1039/c9se00479c.

[73] M. Delpierre, "An ex-ante LCA study on wind-based hydrogen production in the Netherlands," *TU Delft Technology, Policy and Management*, no. August, 2019, [Online]. Available: https://repository.tudelft.nl/islandora/object/uuid%3Afc89a24e-9ef8-49cf-b5fb-3f3fa1e3051b.

[74] National Institute for Public Health and the Environment, "LCIA: the ReCiPe model | RIVM," 2018. https://www.rivm.nl/en/life-cycle-assessment-lca/recipe (accessed Jun. 01, 2021).

[75] T. Sonderegger and N. Stoikou, "Implementation of life cycle impact assessment methods in the ecoinvent database v3.9 and v3.9.1.".

[76] IEAGHG, "Biomass and CCS – Guidance for accounting for negative emissions," 2014.

[77] AACE International, "Recommended Practice No. 18R-97: Cost Estimate Classification System, Rev March 1, 2016," p. 10, 2016, [Online]. Available: http://www.aacei.org/toc/toc_18R-97.pdf.

[78] Lamers P, Tan ECD, Searcy EM, Scarlata CJ, Cafferty KG, Jacobson JJ. Strategic supply system design - a holistic evaluation of operational and production cost for a biorefinery supply chain. *Biofuels Bioprod Biorefin* 2015;9(6):648–60. https://doi.org/10.1002/bbb.1575.

[79] GOV.UK, "Energy Security Bill factsheet: Network charging compensation scheme for energy intensive industries (added 9 May 2023)," May 29, 2023. https://www.gov.uk/government/publications/energy-security-bill-factsheets/energy-security-bill-factsheet-network-charging-compensation-scheme-for-energy-intensive-industries (accessed Jun. 14, 2023).

[80] NREL, "Wind LCA Harmonization," vol. 2012, no. Awea, p. 2, 2013, doi: 10.1111/j.1530-9290.2012.00464.x/pdf.National.

[81] Pietra A, Gianni M, Zuliani N, Malabotti S, Taccani R. Experimental characterization of an alkaline electrolyser and a compression system for hydrogen production and storage. *Energies (basel)* 2021;14(17):1–17. https://doi.org/10.3390/en14175347.

[82] Abdin Z, Webb CJ, Gray EMA. Modelling and simulation of an alkaline electrolyser cell. *Energy* 2017;138:316–31. https://doi.org/10.1016/j.energy.2017.07.053.

[83] Kojima H, Matsuda T, Matsumoto H, Tsujimura T. Development of dynamic simulator of alkaline water electrolyzer for optimizing renewable energy systems. *Journal of International Council on Electrical Engineering* 2018;8(1):19–24. https://doi.org/10.1080/22348972.2018.1436931.

[84] Tijani AS, Yusup NAB, Rahim AHA. Mathematical modelling and simulation analysis of advanced alkaline electrolyzer system for hydrogen production. *Procedia Technol* 2014;15:798–806. https://doi.org/10.1016/j.protcy.2014.09.053.

[85] Tighe S. Guidelines for Probabilistic Pavement Life Cycle Cost Analysis. *Transportation Research Record: Journal of the Transportation Research Board* 2001;1769(1):28–38. https://doi.org/10.3141/1769-04.

[86] M. M. Ramirez-Corredores, "Sustainable production of CO2-derived materials," *npj Materials Sustainability*, vol. 2, no. 1, p. 35, Oct. 2024, doi: 10.1038/s44296-024-00041-9.

[87] Ghiat I, Mahmood F, Govindan R, Al-Ansari T. CO2 utilisation in agricultural greenhouses: A novel 'plant to plant' approach driven by bioenergy with carbon capture systems within the energy, water and food Nexus. *Energy Convers Manag* 2021;228:113668. https://doi.org/10.1016/j.enconman.2020.113668.

[88] Wang W, Rao L, Wu X, Wang Y, Zhao L, Liao X. Supercritical carbon dioxide applications in food processing. *Food Eng Rev* 2021;13(3):570–91. https://doi.org/10.1007/s12393-020-09270-9.

[89] Al-Shargabi M, Davoodi S, Wood DA, Rukavishnikov VS, Minaev KM. Carbon Dioxide Applications for Enhanced Oil Recovery Assisted by Nanoparticles: Recent Developments. *ACS Omega* 2022;7(12):9984–94. https://doi.org/10.1021/acsomega.1c07123.

[90] M. Marchese, N. Heikkinen, E. Giglio, A. Lanzini, J. Lehtonen, and M. Reinikainen, "Kinetic study based on the carbide mechanism of a co-pt/γ-al2 o3 fischer–tropsch catalyst tested in a laboratory-scale tubular reactor," *Catalysts*, vol. 9, no. 9, 2019, doi: 10.3390/catal9090717.

[91] E4Tech, "Review of Technologies for Gasification of Biomass and Wastes Final report," *NNFCC The Bioeconomy Consultants*, no. June, pp. 1–130, 2009, [Online]. Available: http://www.e4tech.com/wp-content/uploads/2016/01/gasification2009.pdf%0Ahttp://www.nnfcc.co.uk/tools/review-of-technologies-for-gasification-of-biomass-and-wastes-nnfcc-09-008.
[92] IATA, "IATA - Fuel Price Monitor," 2021. https://www.iata.org/en/publications/economics/fuel-monitor/ (accessed Apr. 28, 2021).
[93] S. Majer, K. Oehmichen, D. Moosmann, H. S. Dbfz, K. Sailer, M. Matosic, *et al.*, "D5 . 1 Assessment of integrated concepts and identification of key factors and drivers," 2021.
[94] TransportPolicy.net, "US: Fuels: Renewable Fuel Standard | Transport Policy." https://www.transportpolicy.net/standard/us-fuels-renewable-fuel-standard/ (accessed Dec. 20, 2021).
[95] Schyns JF, Booij MJ, Hoekstra AY. The water footprint of wood for lumber, pulp, paper, fuel and firewood. *Adv Water Resour* 2017;107:490–501. https://doi.org/10.1016/j.advwatres.2017.05.013.
[96] Pan S-Y, Snyder SW, Packman AI, Lin YJ, Chiang P-C. Cooling water use in thermoelectric power generation and its associated challenges for addressing water-energy nexus. *Water-Energy Nexus* 2018;1(1):26–41. https://doi.org/10.1016/j.wen.2018.04.002.
[97] Department for Transport, "Supporting the transition to Jet Zero: Creating the UK SAF Mandate- Government response to the second consultation on the SAF Mandate," 2024. [Online]. Available: www.gov.uk/government/organisations/.
[98] E. and I. S. Department for Business, "Net Zero Strategy: Build Back Greener," 2021.
[99] Department for Transport, "Sustainable aviation fuels mandate: Summary of consultation responses and government response," no. July 2022, 2022, [Online]. Available: www.gov.uk/government/organisations/.
[100] Department For Transport, "Sustainable aviation fuels mandate: A consultation on reducing the greenhouse gas emissions of A consultation on reducing the greenhouse gas emissions of aviation fuels in the UK greenhouse gas emissions of aviation fuels in the UK," no. July, 2021, [Online]. Available: https://assets.publishing.service.gov.uk/government/uploads/system/uploads/attachment_data/file/1005382/sustainable-aviation-fuels-mandate-consultation-on-reducing-the-greenhouse-gas-emissions-of-aviation-fuels-in-the-uk.pdf.